Supplemental Figure 1. Analysis of ECM1 expression in sc/snRNA-seq of cardiac interstitial cells from healthy human hearts.[1] UMAP and violin plots of ECM1 expression levels in specific cardiac cell-sub populations: fibroblasts (A), leukocytes (B), and vascular cells (C). ECM1 positive cells are displayed as a blue overlay on grey total cell identity UMAP coordinates.

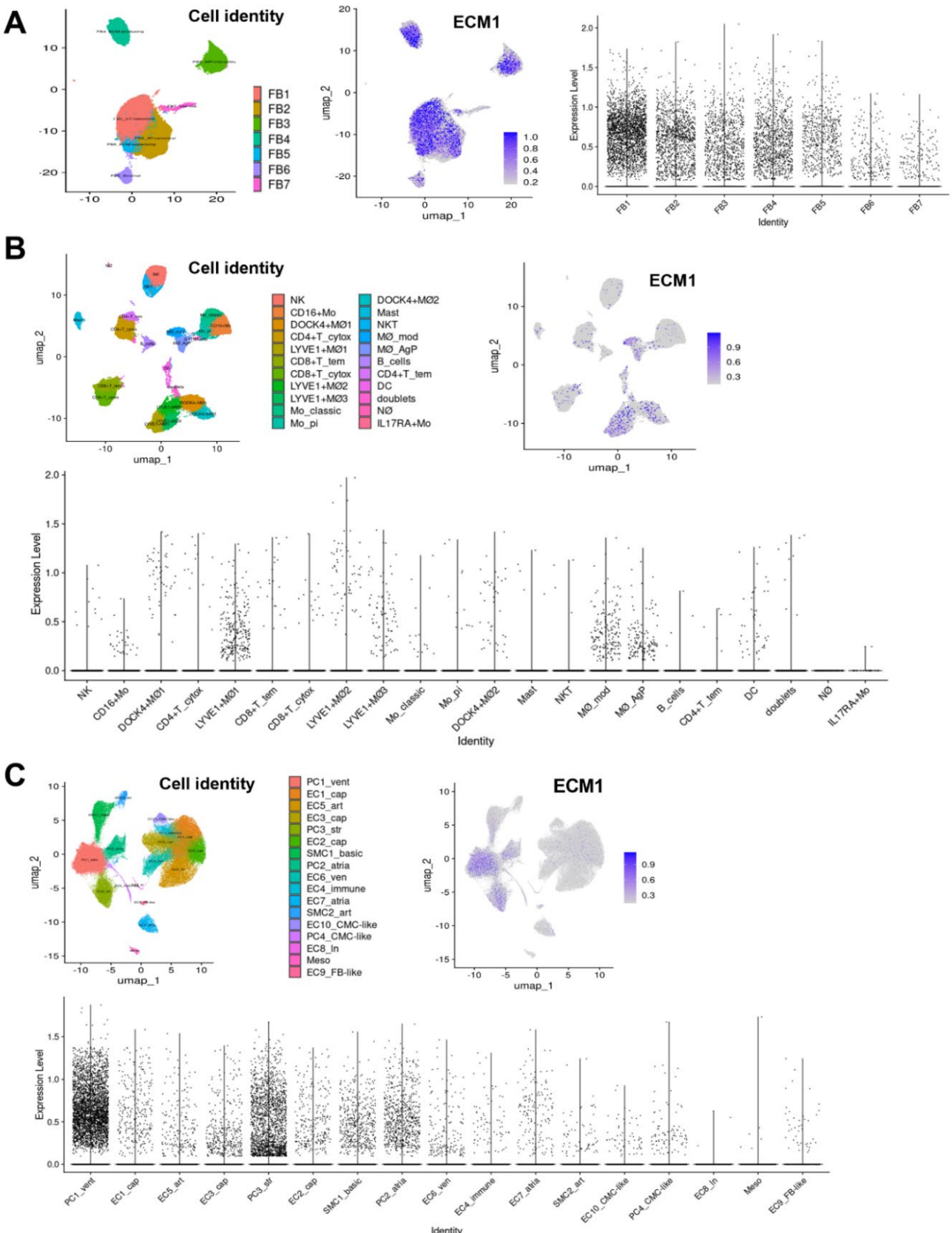

Supplemental Figure 2. Analysis of ECM1 expression in human dilated cardiomyopathy and sc/snRNA-seq of cardiac interstitial cells from mouse hearts post-TAC.[2] A) Immunohistochemistry of ECM1 protein expression in the human heart with dilated cardiomyopathy (DCM) shows ECM1 expression is predominantly interstitial, localized to fibrotic and peri-vascular areas (40x magnification). B-C) UMAP and violin plots of ECM1 expression levels in specific cardiac cell-sub populations in sham and post-TAC, including fibroblasts (cluster 0) and macrophages (cluster 1) and endothelial cells (clusters 2-5 & 13). D) ECM1 positive cells are displayed as a red overlay on grey total cell identity UMAP coordinates. E) violin plots of ECM1 expression levels in specific cardiac cell-sub populations in sham and post-TAC. F) A column graph showing ECM1+ cell numbers increase in fibroblast (CFb) and macrophage (MΦ) clusters post-TAC, relative to sham.

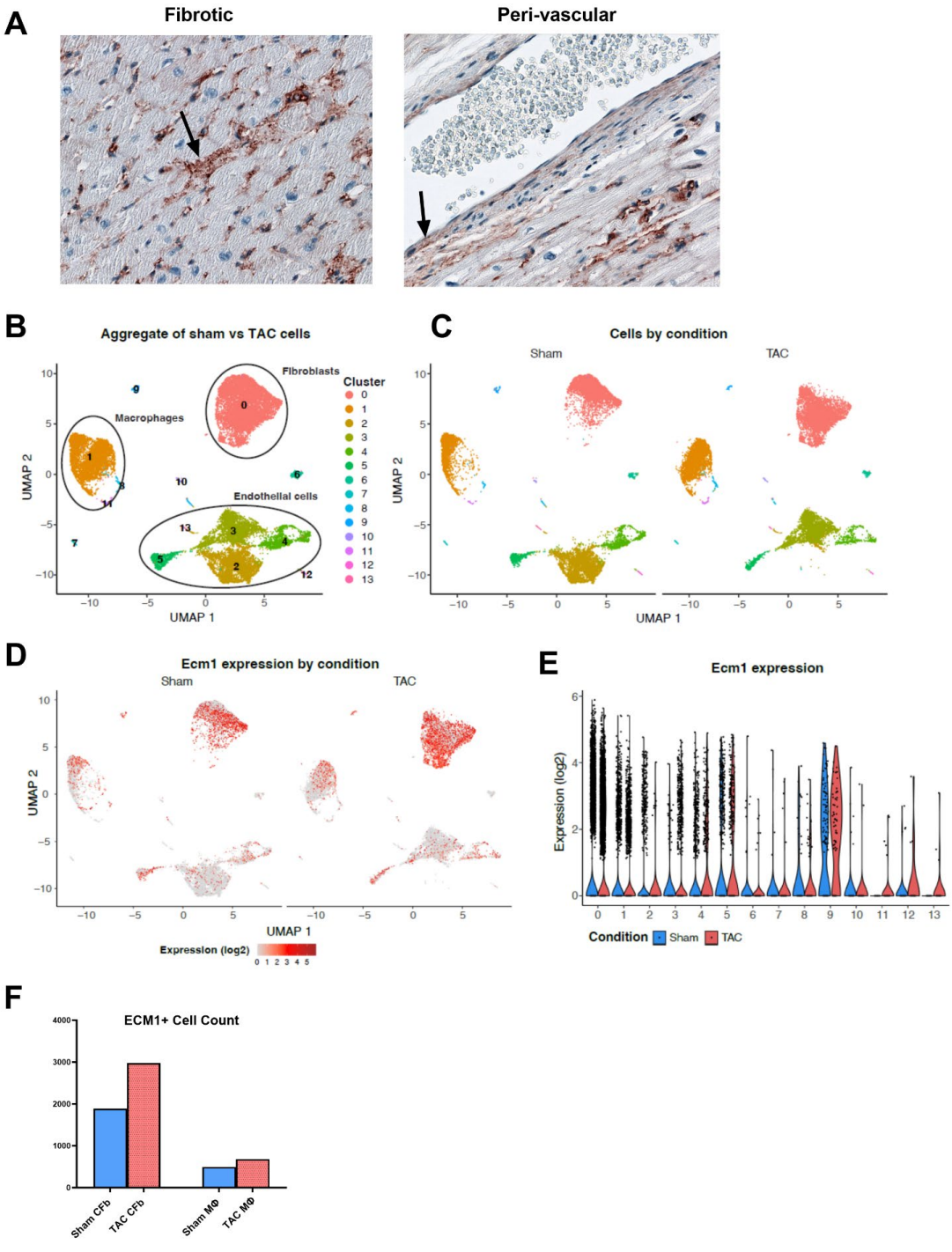
A
Fibrotic
Peri-vascular
B
Aggregate of sham vs TAC cells
Fibroblasts
Macrophages
Endothelial cells
Cluster
UMAP 1
UMAP 2
C
Cells by condition
Sham
TAC
D
Ecm1 expression by condition
Expression (log2)
E
Ecm1 expression
Expression (log2)
Condition Sham TAC
F
ECM1+ Cell Count
Sham CFb
TAC CFb
Sham MΦ
TAC MΦ

Supplemental Figure 3. ECM1 activates Rac1,2,3 activity, and co-localizes with and phosphorylates CTNND1. A) G-LISA assay showed ECM1 treatment (20ng/ml) for 10min significantly increased Rac1,2,3 activity (p=0.037); presented as mean ± SD, assessed via Student's T-test n=6/group. B) Immunofluorescence of HuCFb cells in culture showed ECM1 co-localizes with CTNND1 (40x magnification zoomed in), arrowhead shows an example area of interest. C) Western blotting showed ECM1 treatment (20ng/ml) for 10min significantly increased CTNND1 phosphorylation at serine 268 (left) and 252 (right) (assessed as the ratio of phosphorylated/total CTNND1); presented as mean ± SD, assessed via Student's T-test n=6/group. F) *p<0.05; ***p<0.001; ****p<0.0001.

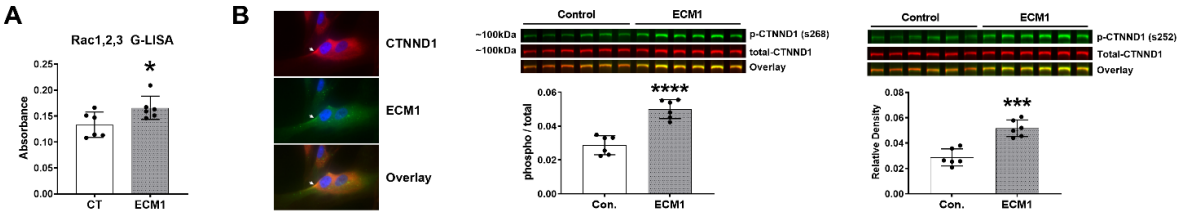

Supplemental Table 1: Percentage of major cell types which contribute to total interstitial cell number in human heart (excluding myocytes).[1]

Cell type	**Percentage of total cells in dataset**
Adi (adipocytes)	0.78
EC (endothelial cells)	20.69
FB (fibroblasts)	12.21
Total Leukocytes	8.41
Meso (mesothelial cells)	0.15
NC (neuronal cells)	0.81
PC (pericytes)	16.02
SMC (smooth muscle cells)	3.34

Supplemental Table 2: Characteristics of the most prominent ECM1 expressing human cardiac cell populations. Cell characteristics are as previously described.[1]

Fibroblast populations	
FB1 (VT-canonical)	regional enrichment in ventricles (left, right, apex and interventricular septum). Express canonical genes and define a basal, chamber-specific FB expression program FB1, FB4–FB6 are enriched in the ventricles
FB2 (AT-canonical)	regional enrichment in atria (left and right). FB2 cells express canonical genes and define a basal, chamber-specific FB expression program.
FB3 (macrophage/MP-interacting)	regional enrichment in atria (left and right). FB3 are less abundant in the left ventricle, have lower expression of ECM-related genes but higher expression of cytokine receptors such as OSMR and ILST643. These distinctive fibroblast gene programs probably govern stress-responsive cardiac remodeling and contribute to homeostasis. Also enriched for oncostatin M pathway compared to other FB populations.
FB4 (ECM-producing)	Enriched in the ventricles (left, right, apex and interventricular septum). Less abundant in the right atrium than other regions. Express genes responsive to TGFβ signaling (for example, POSTN and TNC)
FB5 (ECM-organizing)	Enriched in the ventricles (left, right, apex and interventricular septum). Less abundant in the right atrium than other regions. Have higher expression of genes involved in the production, remodeling and degradation of extracellular matrix (ECM).
Leukocyte populations	
LYVE1+MØ1	Cardiac monocyte-derived macrophages. Enriched in clathrin and cathepsin genes. Related to recently described tissue-resident macrophages associated with cardiovascular remodeling, although they are negative for TIMD4.
MØ_mod (monocyte derived macrophages)	Monocyte-derived macrophages. Express LYVE1 and FOLR2, monocyte-like markers CEBPB and S100A8, and chemoattractant cytokine genes CCL13 and CCL18.
MØ_AgP (antigen presenting macrophages)	Antigen-presenting macrophages are FOLR2−, LYVE1− and MERTK−, and enrich for HLA-DRA, HLA-DMA, HLA-DMB, HLA-DPA1 and TREM2 (described in lipid-associated macrophages).
LYVE1+MØ2	Similar to LYVE1+MØ1, except not necessarily cardiac monocyte-derived. Enriched in clathrin and cathepsin genes. Related to recently described tissue-resident macrophages associated with cardiovascular remodeling, although they are negative for TIMD4.
LYVE1+MØ3	Similar to LYVE1+MØ1 andLYVE1+MØ2, except LYVE1+MØ3 are enriched for HLA-DOA, HLA-DQA1/2 and HLA-DQB1. Also related to recently described tissue-resident macrophages associated with cardiovascular remodeling, although negative for TIMD4.
Vascular populations	
PC1_vent (ventricle-enriched pericytes)	Enriched in ventricles. Enriched for adhesion molecules (NCAM2 and CD38), and CSPG4, which is involved in microvascular morphogenesis and EC cross-talk
PC3_str (stromal pericytes)	Co-express pericyte markers and very low levels of pan-EC transcripts. RNA velocity analyses suggest a directionality that indicates PC3_str cells as a transitional state between pericytes and ECs (Extended Data Fig. 4h, i). These observations may relate to bidirectional pericyte or endothelial cell (trans)differentiation, which remains controversial
PC2_atria (atria-enriched pericytes)	Enriched in the atria and express a similar profile of adhesion molecules as PC1_vent.

SMC1_basic	Vascular SMCs that express MYH11, express transcripts that indicate immaturity, including the stem-cell marker LGR6 (Barker and Clevers, 2010), and proliferation-associated RGS5 (Daniel et al., 2016). SMC1_basic may be venous-derived (Vanlandewijck et al., 2018).

Supplemental Table 3: Most prominent ECM1 expressing cell population metadata (not including expression level).[1]

	Cell type	ECM1 negative	ECM1 positive	total # cells	% ECM1+	cell type as a % of all cells	ECM1+ cells as % of all cells
Fibroblasts	FB1_VT-canonical	24075	2557	26632	9.6012	5.48	0.53
	FB2_AT-canonical	12517	1262	13779	9.1589	2.83	0.26
	FB4_ECM-producing	5079	1067	6146	17.3609	1.26	0.22
	FB3_MP-interacting	6854	890	7744	11.4928	1.59	0.18
	FB5_ECM-organising	1935	583	2518	23.1533	0.52	0.12
	FB6_Stromal	1383	227	1610	14.0994	0.33	0.05
	FB7_CM-like	756	156	912	17.1053	0.19	0.03
	Combined Fibroblasts		6742	59341	11.3615	12.21	1.39
	Cell type	**ECM1 negative**	**ECM1 positive**	**total # cells**	**% ECM1+**	**cell type as a % of all cells**	**ECM1+ cells as % of all cells**
Vascular Cells	PC1_vent	46535	3560	50095	7.1065	10.30	0.73
	PC3_str	12385	1846	14231	12.9717	2.93	0.38
	PC2_atria	10609	714	11323	6.3057	2.33	0.15
	SMC1_basic	12623	491	13114	3.7441	2.70	0.10
	EC3_cap	16528	369	16897	2.1838	3.48	0.08
	EC1_cap	27134	283	27417	1.0322	5.64	0.06
	EC2_cap	13171	274	13445	2.0379	2.77	0.06
	EC5_art	20122	195	20317	0.9598	4.18	0.04
	EC6_ven	8316	170	8486	2.0033	1.75	0.03
	EC7_atria	4327	158	4485	3.5229	0.92	0.03
	PC4_CMC-like	2114	93	2207	4.2139	0.45	0.02
	EC4_immune	5560	77	5637	1.3660	1.16	0.02
	SMC2_art	3060	68	3128	2.1739	0.64	0.01
	EC10_CMC-like	2547	61	2608	2.3390	0.54	0.01
	EC9_FB-like	491	42	533	7.8799	0.11	0.01
	Meso	712	6	718	0.8357	0.15	0.00
	EC8_ln	751	3	754	0.3979	0.16	0.00
	Combined Vascular Cells		8410	195395	4.3041	40.19	1.73
	Cell type	**ECM1 negative**	**ECM1 positive**	**total # cells**	**% ECM1+**	**cell type as a % of all cells**	**ECM1+ cells as % of all cells**
Leukocytes	LYVE1+MØ	2762	256	3018	8.4824	0.62	0.05
	MØ_mod	1141	172	1313	13.0998	0.27	0.04
	MØ_AgP	1135	143	1278	11.1893	0.26	0.03
	LYVE1+MØ3	1871	86	1957	4.3945	0.40	0.02
	LYVE1+MØ2	2029	59	2088	2.8257	0.43	0.01
	DOCK4+MØ1	3188	51	3239	1.5746	0.67	0.01

	DC	769	45	814	5.52823	0.17	0.01
	DOCK4+MØ2	1586	40	1626	2.4600	0.33	0.01
	CD16+Mo	3247	31	3278	0.9457	0.67	0.01
	CD8+T_tem	2977	24	3001	0.7997	0.62	0.00
	Mo_classic	1867	16	1883	0.8497	0.39	0.00
	CD8+T_cytox	2941	15	2956	0.5074	0.61	0.00
	CD4+T_cytox	3099	14	3113	0.4497	0.64	0.00
	Mo_pi	1640	12	1652	0.7264	0.34	0.00
	NK	3617	11	3628	0.3032	0.75	0.00
	doublets	614	9	623	1.4446	0.13	0.00
	CD4+T_tem	1041	6	1047	0.5731	0.22	0.00
	Mast	1538	5	1543	0.3240	0.32	0.00
	NKT	1459	4	1463	0.2734	0.30	0.00
	B_cells	1191	4	1195	0.3347	0.25	0.00
	IL17RA+Mo	31	1	32	3.125	0.01	0.00
	NØ	121	0	121	0	0.02	0.00
	Combined Leukocytes		1004	40868	2.4567	8.41	0.21

Supplemental Table 4: Most prominent ECM1 expressing cell population, specific expression levels.[1]; * = all expression values were multiplied by a factor of 10 to produce larger/more visually interpretable numbers.

Cell type	**average ECM1 expression***
FB5_ECM-organising	2.156545642
FB4_ECM-producing	1.495260315
FB1_VT-canonical	0.985049919
PC3_str	0.9548165
FB3_MP-interacting	0.94968919
FB7_CM-like	0.869133827
FB2_AT-canonical	0.809450903
FB6_Stromal	0.717818108
PC1_vent	0.708297307
MØ_mod	0.696993674
LYVE1+MØ2	0.540295116
EC9_FB-like	0.513880249
PC2_atria	0.511881155
LYVE1+MØ1	0.484529609
MØ_AgP	0.462991062
DC	0.400493194
LYVE1+MØ3	0.380614456
EC7_atria	0.328767895
SMC1_basic	0.259398339
DOCK4+MØ1	0.258763987
DOCK4+MØ2	0.245173465
PC4_CMC-like	0.241680387
EC2_cap	0.155614417
CD8+T_tem	0.120402501
EC3_cap	0.120011558
EC6_ven	0.118434211
SMC2_art	0.103660082
EC1_cap	0.101689835
EC4_immune	0.099793675
EC10_CMC-like	0.097193263
Meso	0.089125168
Mo_pi	0.088484013
IL17RA+Mo	0.086873008
CD4+T_cytox	0.086744052
EC5_art	0.063658103
CD8+T_cytox	0.05822222
Mast	0.055934149
Mo_classic	0.050510158
NKT	0.042248601
CD4+T_tem	0.034450231

CD16+Mo	0.032345739
NK	0.031131977
EC8_ln	0.024524133
B_cells	0.023164137
NØ	0

Supplemental Table 5: Characteristics of most prominent ECM1 expressing mouse cardiac cell sub-populations. Cell characteristics are as described[3] with the exception of MAC8 cells, which we defined here for the first time.

Fibroblast populations	
Fibroblast-Sca1-high (F-SH)	Resident, unactivated fibroblast population, most prominent in sham hearts. Expresses canonical fibroblast markers such as Pdgfra, Pdgfra-GFP, Ddr2 and Col1a1. Contains the highest frequency of Pdgfra and Ly6a(Sca1)-expressing cells, and enriched in S+P+ (SCA1+PDGFRα+) fibroblasts and clonal colony-forming units. Enriched in cardiac colony-forming mesenchymal stromal cell (MSC)-like cells (cCFU-F), which show multi-lineage differentiation and self-renewal in vitro. Characterized by over-representation of genes involved in the biological process (BP) cell adhesion, which included cell surface receptor genes Ackr3(Cxcr-7), Thy1(Cd90), Axl and Cd34.
Fibroblast-Sca1-low (F-SL)	Resident, unactivated fibroblast population, most prominent in sham hearts. Expresses canonical fibroblast markers such as Pdgfra, Pdgfra-GFP, Ddr2 and Col1a1. Characterized by GO BP terms signaling and signal transduction. Within the signal transduction category, majority secreted proteins including APOE, BMP4 and ADM. Thus, F-SL, a major sub-division of fibroblasts, has a unique secretory phenotype distinct from that in F-SH, which is enriched in MSC-like colony forming cells.
Activated fibroblasts (F-Act)	Activated fibroblast population. Express Postn at high levels in ~80% of cells. Express Acta2 in 28% (MI-day 3) and 35% (MI-day 7), much lower levels compared to MYO; suggests a contractile phenotype in some F-Act cells. Most closely related to F-SH & F-SL and is more distant from MYO. F-Act over-represent GOBP terms collagen fibril organization and regulation of wound healing. F-Act top upregulated gene is Cilp, encoding a matricellular protein and inhibitor of TGF-β1 signaling, consistent with F-Act being a pre-MYO population in which fibrosis is constrained. F-Act acts as an intermediary population for MYO, as it expands by proliferation up to MI-day 3 and differentiates to MYO during the transition from MI-day 3 to MI-day 7.
Myofibroblasts (Myo)	Activated fibroblasts. Represent 11.49% of total interstitial cells at MI-day 7; 2nd most populous cell type to M2MΦ at day 7. Express fibrogenic (e.g. Periostin; POSTN) and/or contractile (e.g. αSmooth Muscle Actin; αSMA) proteins. Show strong upregulation of numerous collagen genes (e.g. Col1a1, Col3a1, Col5a2), Postn (99.5%) and Acta2 (61%). Upregulated genes involved in wound healing and cell migration including Fn(Fibronectin) and Cthrc1(Collagen Triple Helix Repeat Containing I). Have decreased expression of Pdgfra, Pdgfra-GFP, Ly6a(Sca1), Thy1(Cd90) and Cd34, indicating loss of stem/progenitor cell markers. GOBP terms are collagen fibril organization and cell adhesion, containing collagen genes Col3a1, Col5a1, Col11a1 and Col14a1, and others involved in cell:cell and cell:matrix adhesion including Thbs1 (encoding Thrombospondin 1) and Fbn1. Other terms included angiogenesis and heart development as well as negative regulation of canonical Wnt signaling pathway.
(F-WntX)	Characterised by an anti-WNT, anti-CTGF and anti-TGF-β extracellular and intracellular signaling milieu. Expressed Postn(Periostin), Acta2(αSMA), Tagln(Transgelin) and Scx(Scleraxis), in both sham and MI conditions, suggesting an activated state even in the absence of injury. Top upregulated gene was Wif1, encoding a secreted canonical WNT pathway inhibitor essential for cardiac repair after MI (Meyer et al., 2017). WIF1 can also antagonize Connective Tissue Growth Factor (CTGF) signaling (Surmann-Schmitt et al., 2012), which plays a supportive role in cardiac fibrosis (Travers et al., 2016). Wif1 was almost uniquely expressed in F-WntX in all conditions. Multiple other WNT pathway-related genes were upregulated encoding WNT ligands (WNT5a, WNT16), soluble WNT antagonists (DKK3, SFRP2), membrane-bound WNT receptor (FRZB) and AXIN2, a component of the β-catenin destruction complex. F-WntX also showed upregulated Fmod,

	which inhibits fibrillogenesis and sequesters pro-fibrotic factor TGF-β within ECM. Overall, this signature suggests an anti-WNT, anti-CTGF and anti-TGF-β extracellular and intracellular signaling milieu for F-WntX cells.
Leukocyte populations	
Cardiac tissue resident macrophages (MAC-TR)	Cardiac tissue-resident MΦ. Have a cell signature of Cx3cr1high Adgre1(F4/80)high H2-Aa(MHC-II)+ Itgam(CD11b)low Ly6c2low Ccr2-. Upregulated pro-regenerative genes Igf1 and Pdgfb/c.
M1 macrophages (M1MØ)	Classical inflammatory monocyte-derived M1 macrophages (M1MΦ). One of the most abundant cell types at MI day 3. Express a cell signature of Ccr2high Adgre1(F4/80)+ Ly6c2+ H2-Aa(MHC-II)+. Also express additional MΦ markers including Mertk and C1q. Hierarchical clustering shows M1MΦ are most closely related to M1 monocytes. Differentially expressed genes show over-representation in GO terms for leukocyte migration and responses to interleukin-1.
M2 macrophages (M2MØ)	Non-classical M2 MΦ involved in inflammation resolution and repair, and the most prominent population at MI-day 7; M2MΦ population increases late during injury repair from <2% of TIP in sham and MI-day 3 hearts, to 16% at MI-day 7. Closely related to tissue-resident macrophages (MAC-TR). Express a cell signature of Ccr2high Adgre1(F4/80)+ H2-Aa(MHC-II)high Ly6c2-. Also express Cx3cr1, and have upregulated pro-regenerative genes Igf1 and Pdgfb/c. The majority of M2MΦ were Ccr2high (important for migration); however, a minor sub-population was Ccr2low and these expressed the highest levels of Igf1 and lower levels of MHC-II. Differentially expressed genes show over-representation of show GO term antigen presentation via MHC class II.
M1 monocytes (M1Mo)	Classical blood-derived M1 monocytes (M1Mo). Characterized by the expression signature Adgre1(F4/80)+ Itgam(CD11b)+ Fcgr1(CD64)+ Ly6c2high Ccr2high H2-Aa(MHC-II)low. Also characterized by having lower size and granularity than MΦ, and lower levels of MΦ markers Adgre(F4/80), Itgam(CD11b) and H2-Aa(MHC-II). At MI-day 3 M1Mo are also low or negative for the MΦ markers Siglec1, Mrc1, Maf, Trem2 and Mertk (involved in phagocytosis), and C1 complement genes C1qa, b and c which are involved in recruitment of new inflammatory cells and protection against autoimmunity (in addition to complement fixation). Differentially expressed genes show over-representation of GO terms for cell migration, inflammation and T cell activation.
(MAC8)	Differentially expressed genes show over-representation in GO terms for inflammatory response and regulation of response to external stimulus. When MAC8 marker genes greater than 1.25-fold upregulated against all other cells were subject to GOnet enrichment, there is an over-representation of GOBP response to stimulus, inflammatory response and myeloid leukocyte/neutrophil/granulocyte/neutrophil cell migration or chemotaxis/locomotion; the top GOMF term was signaling receptor binding. Suggesting a responsive, cell phenotype most notably associated with paracrine signaling and migratory/chemotactic or locomotive effects.
interferon-responsive gene expressing macrophages (MAC-IFNIC)	Macrophages that express interferon-responsive genes (MAC-IFNIC). Showed strong upregulation of interferon (IFN)-induced genes including Ifit3, Ifit1 and Cxcl10. GO term analysis implicate responses to IFN α, β, and γ. Appear to arise from Ccr2+ MΦ as opposed to monocytes, and likely correspond to the recently described inflammatory MΦ subtype that has negative effects on heart repair after MI through promotion of inflammatory cell types, and cytokine and chemokine expression (King et al., 2017).
Vascular populations	
EC1	The majority EC1 population (encompass the largest number of ECs at all time-points) express Ly6a (encodes SCA1) as well as the vascular transcription factor (TF) Sox17, and likely represents microvascular ECs.

EC2	EC2 expressed canonical arterial endothelial markers such as Bmx, Sema3g and Efnb2, as well as TF genes Sox17 and Hey1, the latter acting downstream of NOTCH which is required for arterial EC fate.
EC3	EC3 almost uniquely expressed venous EC marker Nr2f2 (encoding COUPTFII) and Von Willebrand factor (Vwf), and a minority (~3%) expressed Prox1 and Lyve1, consistent with a lymphatic identity.
Mural (contains pericytes)	Mural cells which also encompass pericytes. Characterized as Cspg4+ Pdgfrb+, and a new lineage marker, Vtn, encoding Vitronectin, was specifically expressed in these mural cells

Supplemental Table 6: All ECM1 specific cell expression metadata of interstitial cell populations. Data is separated by time-point post-MI and ranked by percentage of ECM1+ cells within each sub-population.[3]

Rank	Cluster	Condition	log 2_mean ECM1 expression	ECM1+ Cell #	Total Cell #	% total cells at time	% cells ECM1+	ECM1+ cells as % of total cells at time
1	MYO	Sham	2.2385	22	22	0.3844	100.00	0.38
2	MAC8	Sham	2.9702	13	13	0.2272	100.00	0.23
3	F-SH	Sham	2.7406	576	657	11.4800	87.67	10.06
4	F-Act	Sham	2.6191	478	553	9.6628	86.44	8.35
5	F-WntX	Sham	2.1573	75	96	1.6774	78.13	1.31
6	M1MΦ	Sham	1.4476	2	3	0.0524	66.67	0.03
7	MAC-IFNIC	Sham	0.9455	2	3	0.0524	66.67	0.03
8	F-SL	Sham	1.8824	879	1348	23.5541	65.21	15.36
9	M2MΦ	Sham	1.0610	15	26	0.4543	57.69	0.26
10	Mural	Sham	1.5439	79	184	3.2151	42.93	1.38
11	M1Mo	Sham	0.8692	15	40	0.6989	37.50	0.26
12	EC3	Sham	1.2754	69	229	4.0014	30.13	1.21
13	DC	Sham	0.8125	7	24	0.4194	29.17	0.12
14	MAC-TR	Sham	0.7461	38	159	2.7783	23.90	0.66
15	EC2	Sham	0.9342	54	241	4.2111	22.41	0.94
16	Cyc	Sham	0.6719	8	37	0.6465	21.62	0.14
17	Glial	Sham	0.3270	3	18	0.3145	16.67	0.05
18	EC1	Sham	0.6829	188	1215	21.2301	15.47	3.28
19	MAC6	Sham	0.5584	5	33	0.5766	15.15	0.09
20	TC1-Cd8	Sham	0.4170	23	152	2.6559	15.13	0.40
21	MAC7	Sham	0.4016	5	44	0.7688	11.36	0.09
22	NKC	Sham	0.4617	4	48	0.8387	8.33	0.07
23	TC2-Cd4	Sham	0.2634	10	132	2.3065	7.58	0.17
24	BC	Sham	0.2678	23	446	7.7931	5.16	0.40
			Cell Group	**total ECM1+ Cell #**	**Total Cell #**	**Cell number as % of cells at time**	**ECM1+ cells as % of cells at time**	**% of "cell group" ECM1+ at this time**
				2593	5723			
			Total Fibroblast	2030	2676	46.7587	35.4709	75.8595
			Total Mo/MΦ	95	321	5.6089	1.6600	29.5950
			Total EC	311	1685	29.4426	5.4342	18.4570

Rank	Cluster	Condition	log 2_mean ECM1 expression	ECM1+ Cell #	Total Cell #	% total cells at time	% cells ECM1+	ECM1+ cells as % of total cells at time
1	MAC8	MI-day 3	2.6895	86	106	2.7355	81.13	2.22
2	MYO	MI-day 3	2.1545	3	4	0.1032	75.00	0.08
3	F-SH	MI-day 3	2.2669	17	25	0.6452	68.00	0.44
4	F-SL	MI-day 3	1.9149	27	40	1.0323	67.5	0.70
5	M1MΦ	MI-day 3	2.2011	1288	1964	50.6839	65.58	33.24
6	M2MΦ	MI-day 3	1.5824	32	49	1.2645	65.31	0.83
7	F-WntX	MI-day 3	1.6874	5	8	0.2065	62.50	0.13
8	MAC-IFNIC	MI-day 3	1.9108	78	125	3.2258	62.40	2.01
9	F-Act	MI-day 3	1.8295	110	185	4.7742	59.46	2.84
10	Cyc	MI-day 3	0.9515	27	71	1.8323	38.03	0.70
11	M1Mo	MI-day 3	1.0642	151	493	12.7226	30.63	3.90
12	MAC6	MI-day 3	1.0023	30	110	2.8387	27.27	0.77
13	Mural	MI-day 3	0.5939	2	10	0.2581	20.00	0.05
14	EC2	MI-day 3	0.9353	7	37	0.9548	18.92	0.18
15	MAC-TR	MI-day 3	0.4140	4	23	0.5935	17.39	0.10
16	EC3	MI-day 3	0.6381	13	75	1.9355	17.33	0.34
17	EC1	MI-day 3	0.7319	23	162	4.1806	14.20	0.59
18	MAC7	MI-day 3	0.5208	6	43	1.1097	13.95	0.15
19	TC2-Cd4	MI-day 3	0.7320	2	16	0.4129	12.50	0.05
20	TC1-Cd8	MI-day 3	0.6388	3	28	0.7226	10.71	0.08
21	DC	MI-day 3	0.2827	23	271	6.9935	8.49	0.59
22	BC	MI-day 3	0.6780	2	27	0.6968	7.41	0.05
23	NKC	MI-day 3	0.0000	0	2	0.0516	0.00	0.00
24	Glial	MI-day 3	0.0000	0	1	0.0258	0.00	0.00
			Cell Group	**total ECM1+ Cell #**	**Total Cell #**	**Cell number as % of cells at time**	**ECM1+ cells as % of cells at time**	**% of cell group ECM1+ at this time**
				1939	3875			
			Total Fibroblast	162	262	6.7613	4.1806	61.8321
			Total Mo/MΦ	1675	2913	75.1742	43.2258	57.5009
			Total EC	43	274	7.0710	1.1097	15.6934
Rank	**Cluster**	**Condition**	**log 2_mean ECM1 expression**	**ECM1+ Cell #**	**Total Cell #**	**% total cells at time**	**% cells ECM1+**	**ECM1+ cells as % of total**

								cells at time
1	MAC8	MI-day 7	2.3424	18	18	0.4822	100.00	0.48
2	F-WntX	MI-day 7	2.3388	13	15	0.4018	86.67	0.35
3	MYO	MI-day 7	1.7450	371	429	11.4921	86.48	9.94
4	F-SH	MI-day 7	2.5415	142	172	4.6076	82.56	3.80
5	F-Act	MI-day 7	2.1699	301	368	9.8580	81.79	8.06
6	F-SL	MI-day 7	1.9019	189	265	7.0988	71.32	5.06
7	M1MΦ	MI-day 7	1.6169	80	134	3.5896	59.70	2.14
8	Mural	MI-day 7	1.4421	21	39	1.0447	53.85	0.56
9	MAC-IFNIC	MI-day 7	1.1206	14	27	0.7233	51.85	0.38
10	M2MΦ	MI-day 7	1.0189	304	600	16.0729	50.67	8.14
11	EC3	MI-day 7	0.9763	30	102	2.7324	29.41	0.80
12	Cyc	MI-day 7	0.3901	27	108	2.8931	25.00	0.72
13	EC2	MI-day 7	0.8343	22	95	2.5449	23.16	0.59
14	M1Mo	MI-day 7	0.5625	17	79	2.1163	21.52	0.46
15	MAC-TR	MI-day 7	0.7385	9	55	1.4733	16.36	0.24
16	EC1	MI-day 7	0.4262	64	503	13.4744	12.72	1.71
17	MAC6	MI-day 7	0.3280	3	26	0.6965	11.54	0.08
18	DC	MI-day 7	0.1570	9	96	2.5717	9.38	0.24
19	NKC	MI-day 7	0.1701	2	26	0.6965	7.69	0.05
20	TC2-Cd4	MI-day 7	0.2790	6	95	2.5449	6.32	0.16
21	TC1-Cd8	MI-day 7	0.1440	7	144	3.8575	4.86	0.19
22	BC	MI-day 7	0.0517	6	278	7.4471	2.16	0.16
23	MAC7	MI-day 7	0.0472	1	54	1.4466	1.85	0.03
24	Glial	MI-day 7	0.0000	0	5	0.1339	0.00	0.00
			Cell Group	**total ECM1+ Cell #**	**Total Cell #**	**Cell number as % of cells at time**	**ECM1+ cells as % of cells at time**	**% of cell group ECM1+ at this time**
				1656	3733			
			Total Fibroblast	1016	1249	33.4583	27.2167	81.3451
			Total Mo/MΦ	446	993	26.6006	11.9475	44.9144
			Total EC	116	700	18.7517	3.1074	16.5714

Supplemental Table 7: Per-cell Spearman correlation analysis of ECM1 expression against all genes in the mouse scRNAseq dataset.[3]

Rank	Gene name	Spearman_rho	FDR adj. p-value
n/a	Ecm1	1.000	0
1	Lgals1	0.441	0
2	Lrp1	0.435	0
3	Rnase4	0.421	0
4	S100a6	0.402	0
5	Ctsl	0.397	0
6	Pcolce2	0.392	0
7	Dpt	0.389	0
8	Timp2	0.388	0
9	Cfh	0.386	0
10	Fbln1	0.381	0
11	Fxyd1	0.378	0
12	Serping1	0.377	0
13	Ccdc80	0.377	0
14	Entpd2	0.372	0
15	Ptgis	0.371	0
16	Islr	0.371	0
17	Col1a1	0.365	0
18	Cd63	0.365	0
19	Mfap5	0.364	0
20	Col6a1	0.362	0
21	Serpinf1	0.361	0
22	Meg3	0.360	0
23	H2B-EGFP	0.358	0
24	Col1a2	0.357	0
25	Fstl1	0.356	0
26	Loxl1	0.356	0
27	Sod3	0.355	0
28	Sdc2	0.355	0
29	Igfbp6	0.355	0
30	Sfrp1	0.354	0
31	Medag	0.352	0
32	Pmp22	0.352	0
33	Lum	0.351	0
34	Cygb	0.351	0
35	Col6a2	0.350	0
36	Ogn	0.349	0
37	Mmp2	0.349	0
38	Tnxb	0.348	0
39	Clec3b	0.348	0
40	Ahnak2	0.346	0
41	Mxra8	0.346	0

42	Serpine2	0.346	0
43	Htra3	0.345	0
44	Axl	0.345	0
45	Lhfp	0.344	0
46	Gas1	0.344	0
47	Prelp	0.343	0
48	Adamts2	0.343	0
49	Gpx3	0.342	0
50	Cpq	0.338	0
51	Emp1	0.338	0
52	Olfml3	0.338	0
53	Rcn3	0.337	0
54	Lpar1	0.335	0
55	Anxa1	0.335	0
56	Pcolce	0.335	0
57	Rbp1	0.334	0
58	Nbl1	0.333	0
59	Igfbp4	0.333	0
60	Bgn	0.333	0
61	Rarres2	0.333	0
62	Fhl1	0.332	0
63	Gpm6b	0.331	0
64	Col3a1	0.330	0
65	Vcan	0.329	0
66	Mmp23	0.327	0
67	Camk2n1	0.325	0
68	Nupr1	0.324	3.95xE-323
69	Pdlim2	0.323	7.39xE-321
70	Fbn1	0.322	2.07xE-318
71	Oaf	0.320	6.26xE-315
72	Nfix	0.320	1.07xE-314
73	Ugp2	0.320	1.79xE-314
74	Pam	0.317	0.00xE+00
75	Qpct	0.317	3.96xE-308
76	Pcsk6	0.317	6.49xE-308
77	Gsn	0.316	3.38xE-307
78	Gfpt2	0.316	5.60xE-307
79	Aspn	0.315	1.37xE-305
80	Bicc1	0.315	4.27xE-304
81	Fbln2	0.314	3.02xE-303
82	Cryab	0.313	2.23xE-301
83	Aebp1	0.312	2.36xE-298
84	Selenbp1	0.311	3.79xE-296
85	Cp	0.311	7.29xE-296

86	Itgb5	0.311	8.03xE-296
87	Crispld2	0.310	1.43xE-295
88	Smoc2	0.309	2.66xE-293
89	Abca8a	0.309	5.44xE-293
90	Lama2	0.309	1.17xE-292
91	Tcf21	0.308	1.77xE-291
92	Matn2	0.308	2.81xE-290
93	Dpep1	0.308	4.57xE-290
94	Adamts5	0.305	1.40xE-284
95	Pi16	0.304	1.37xE-282
96	Mt1	0.304	4.06xE-282
97	Cd248	0.302	4.44xE-279
98	Cd302	0.302	1.00xE-278
99	Pdgfra	0.301	8.41xE-278
100	Lamc1	0.301	1.62xE-277
101	Snhg18	0.301	1.28xE-276
102	Emp3	0.300	2.00xE-274

Supplemental Table 8: GOnet/DICE GOBP enrichment of the top ECM1 Spearman correlated genes (r ≥ 0.3) from the mouse scRNAseq dataset.[3]

	GO_term_ID	GO_term_def	P	P_FDR_adj	NofGenes
1	GO:0030198	extracellular matrix organization	5.23E-18	0	18
2	GO:0043062	extracellular structure organization	5.28E-17	0	18
3	GO:0048513	animal organ development	1.00E-09	3.08E-06	37
4	GO:0030199	collagen fibril organization	1.20E-09	3.08E-06	7
5	GO:0048731	system development	1.40E-09	3.08E-06	44
6	GO:0032502	developmental process	2.50E-09	4.14E-06	51
7	GO:0007275	multicellular organism development	3.10E-09	4.14E-06	47
8	GO:0048856	anatomical structure development	3.40E-09	4.14E-06	49
9	GO:0032963	collagen metabolic process	3.50E-09	4.14E-06	7
10	GO:0009888	tissue development	3.80E-09	4.14E-06	26
11	GO:0007155	cell adhesion	2.32E-08	2.30E-05	17
12	GO:0022610	biological adhesion	2.84E-08	2.58E-05	17
13	GO:0009611	response to wounding	5.48E-08	4.59E-05	12
14	GO:0032060	bleb assembly	8.59E-08	6.69E-05	4
15	GO:0030334	regulation of cell migration	1.26E-07	8.79E-05	17
16	GO:0030155	regulation of cell adhesion	1.34E-07	8.79E-05	15
17	GO:0001501	skeletal system development	1.37E-07	8.79E-05	13
18	GO:0051270	regulation of cellular component movement	1.81E-07	1.10E-04	18
19	GO:0042060	wound healing	1.95E-07	1.12E-04	10
20	GO:2000145	regulation of cell motility	2.60E-07	1.42E-04	17
21	GO:0009966	regulation of signal transduction	4.47E-07	2.32E-04	30
22	GO:0040012	regulation of locomotion	8.00E-07	3.97E-04	17
23	GO:0070208	protein heterotrimerization	9.84E-07	4.66E-04	4
24	GO:0016043	cellular component organization	1.19E-06	5.25E-04	43
25	GO:0048583	regulation of response to stimulus	1.20E-06	5.25E-04	36
26	GO:0051241	negative regulation of multicellular organismal process	1.97E-06	8.25E-04	19
27	GO:0010646	regulation of cell communication	2.22E-06	8.98E-04	32
28	GO:2000146	negative regulation of cell motility	2.41E-06	9.22E-04	9
29	GO:0023051	regulation of signaling	2.45E-06	9.22E-04	32
30	GO:0010810	regulation of cell-substrate adhesion	2.60E-06	9.43E-04	8
31	GO:0022008	neurogenesis	2.70E-06	9.43E-04	22
32	GO:0097435	supramolecular fiber organization	2.77E-06	9.43E-04	11
33	GO:0071840	cellular component organization or biogenesis	3.22E-06	1.06E-03	43
34	GO:0051239	regulation of multicellular organismal process	3.74E-06	1.20E-03	31
35	GO:0042221	response to chemical	3.94E-06	1.23E-03	34
36	GO:0040007	growth	4.34E-06	1.31E-03	11
37	GO:0048585	negative regulation of response to stimulus	5.49E-06	1.58E-03	20
38	GO:0060346	bone trabecula formation	5.52E-06	1.58E-03	3
39	GO:0031589	cell-substrate adhesion	5.85E-06	1.59E-03	7

40	GO:0040011	locomotion	5.86E-06	1.59E-03	17
41	GO:0051271	negative regulation of cellular component movement	6.25E-06	1.59E-03	9
42	GO:2000026	regulation of multicellular organismal development	6.25E-06	1.59E-03	24
43	GO:0030162	regulation of proteolysis	6.27E-06	1.59E-03	13
44	GO:0050817	coagulation	6.89E-06	1.67E-03	6
45	GO:0007596	blood coagulation	6.89E-06	1.67E-03	6
46	GO:0048523	negative regulation of cellular process	7.18E-06	1.70E-03	38
47	GO:0007599	hemostasis	7.63E-06	1.77E-03	6
48	GO:0048869	cellular developmental process	8.51E-06	1.93E-03	34
49	GO:0040013	negative regulation of locomotion	9.28E-06	2.07E-03	9
50	GO:0050793	regulation of developmental process	9.63E-06	2.10E-03	27
51	GO:0030154	cell differentiation	1.09E-05	2.33E-03	33
52	GO:0009653	anatomical structure morphogenesis	1.13E-05	2.34E-03	24
53	GO:0048608	reproductive structure development	1.15E-05	2.34E-03	10
54	GO:0032501	multicellular organismal process	1.16E-05	2.34E-03	52
55	GO:0048705	skeletal system morphogenesis	1.20E-05	2.34E-03	8
56	GO:0045861	negative regulation of proteolysis	1.20E-05	2.34E-03	9
57	GO:0061458	reproductive system development	1.25E-05	2.39E-03	10
58	GO:0030336	negative regulation of cell migration	1.49E-05	2.81E-03	8
59	GO:0090287	regulation of cellular response to growth factor stimulus	1.62E-05	2.99E-03	8
60	GO:0061430	bone trabecula morphogenesis	1.86E-05	3.37E-03	3
61	GO:0048519	negative regulation of biological process	2.08E-05	3.71E-03	40
62	GO:0060325	face morphogenesis	2.17E-05	3.82E-03	4
63	GO:0000904	cell morphogenesis involved in differentiation	2.68E-05	4.58E-03	11
64	GO:0045595	regulation of cell differentiation	2.70E-05	4.58E-03	21
65	GO:0032101	regulation of response to external stimulus	2.73E-05	4.58E-03	14
66	GO:0035295	tube development	3.14E-05	5.19E-03	14
67	GO:0003414	chondrocyte morphogenesis involved in endochondral bone morphogenesis	3.60E-05	5.69E-03	3
68	GO:0003429	growth plate cartilage chondrocyte morphogenesis	3.60E-05	5.69E-03	3
69	GO:0090171	chondrocyte morphogenesis	3.60E-05	5.69E-03	3
70	GO:0060323	head morphogenesis	3.81E-05	5.93E-03	4
71	GO:0016477	cell migration	4.05E-05	6.22E-03	13
72	GO:0003422	growth plate cartilage morphogenesis	4.36E-05	6.52E-03	3
73	GO:0042063	gliogenesis	4.37E-05	6.52E-03	7
74	GO:0051336	regulation of hydrolase activity	4.51E-05	6.64E-03	14
75	GO:0048699	generation of neurons	4.74E-05	6.75E-03	19
76	GO:0060351	cartilage development involved in endochondral bone morphogenesis	4.90E-05	6.75E-03	4
77	GO:0052547	regulation of peptidase activity	4.96E-05	6.75E-03	9

78	GO:0072275	metanephric glomerulus morphogenesis	4.98E-05	6.75E-03	2
79	GO:0072276	metanephric glomerulus vasculature morphogenesis	4.98E-05	6.75E-03	2
80	GO:0072277	metanephric glomerular capillary formation	4.98E-05	6.75E-03	2
81	GO:0030510	regulation of BMP signaling pathway	5.01E-05	6.75E-03	5
82	GO:0032989	cellular component morphogenesis	5.15E-05	6.84E-03	13
83	GO:0032268	regulation of cellular protein metabolic process	5.63E-05	7.33E-03	24
84	GO:0051128	regulation of cellular component organization	5.70E-05	7.33E-03	24
85	GO:0006950	response to stress	5.76E-05	7.33E-03	28
86	GO:0032879	regulation of localization	5.78E-05	7.33E-03	26
87	GO:0085029	extracellular matrix assembly	6.18E-05	7.60E-03	3
88	GO:0000302	response to reactive oxygen species	6.18E-05	7.60E-03	6
89	GO:0000902	cell morphogenesis	6.21E-05	7.60E-03	12
90	GO:0010466	negative regulation of peptidase activity	6.36E-05	7.71E-03	7
91	GO:0030514	negative regulation of BMP signaling pathway	6.68E-05	7.92E-03	4
92	GO:0010517	regulation of phospholipase activity	6.68E-05	7.92E-03	4
93	GO:0006979	response to oxidative stress	7.42E-05	8.69E-03	8
94	GO:0071230	cellular response to amino acid stimulus	7.78E-05	9.02E-03	6
95	GO:0009887	animal organ morphogenesis	8.62E-05	9.89E-03	14
96	GO:0010171	body morphogenesis	8.90E-05	1.01E-02	4
97	GO:0010951	negative regulation of endopeptidase activity	9.40E-05	1.06E-02	6
98	GO:1903034	regulation of response to wounding	9.69E-05	1.06E-02	6
99	GO:0003418	growth plate cartilage chondrocyte differentiation	9.73E-05	1.06E-02	3
100	GO:0003433	chondrocyte development involved in endochondral bone morphogenesis	9.73E-05	1.06E-02	3
101	GO:0097350	neutrophil clearance	9.93E-05	1.06E-02	2
102	GO:0035582	sequestering of BMP in extracellular matrix	9.93E-05	1.06E-02	2
103	GO:0090101	negative regulation of transmembrane receptor protein serine/threonine kinase signaling pathway	1.04E-04	1.10E-02	5
104	GO:0060324	face development	1.09E-04	1.14E-02	4
105	GO:0008285	negative regulation of cell population proliferation	1.11E-04	1.15E-02	11
106	GO:0034614	cellular response to reactive oxygen species	1.13E-04	1.16E-02	5
107	GO:0010812	negative regulation of cell-substrate adhesion	1.16E-04	1.17E-02	4
108	GO:0043200	response to amino acid	1.16E-04	1.17E-02	6
109	GO:0120036	plasma membrane bounded cell projection organization	1.18E-04	1.18E-02	14
110	GO:0048589	developmental growth	1.21E-04	1.20E-02	9

111	GO:0070206	protein trimerization	1.24E-04	1.22E-02	4
112	GO:0007399	nervous system development	1.33E-04	1.30E-02	22
113	GO:0048565	digestive tract development	1.38E-04	1.33E-02	5
114	GO:0070613	regulation of protein processing	1.40E-04	1.33E-02	4
115	GO:0070887	cellular response to chemical stimulus	1.41E-04	1.33E-02	24
116	GO:0060343	trabecula formation	1.44E-04	1.34E-02	3
117	GO:0046688	response to copper ion	1.44E-04	1.34E-02	3
118	GO:0060284	regulation of cell development	1.50E-04	1.37E-02	14
119	GO:1901701	cellular response to oxygen-containing compound	1.50E-04	1.37E-02	14
120	GO:0030308	negative regulation of cell growth	1.51E-04	1.37E-02	6
121	GO:1903317	regulation of protein maturation	1.58E-04	1.41E-02	4
122	GO:0051674	localization of cell	1.59E-04	1.41E-02	13
123	GO:0048870	cell motility	1.59E-04	1.41E-02	13
124	GO:0006928	movement of cell or subcellular component	1.63E-04	1.43E-02	16
125	GO:0036072	direct ossification	1.65E-04	1.43E-02	2
126	GO:0001957	intramembranous ossification	1.65E-04	1.43E-02	2
127	GO:0007162	negative regulation of cell adhesion	1.72E-04	1.48E-02	7
128	GO:0051246	regulation of protein metabolic process	1.79E-04	1.53E-02	24
129	GO:0060536	cartilage morphogenesis	1.82E-04	1.54E-02	3
130	GO:0050866	negative regulation of cell activation	1.93E-04	1.61E-02	6
131	GO:0010721	negative regulation of cell development	1.96E-04	1.62E-02	8
132	GO:0043933	protein-containing complex subunit organization	1.96E-04	1.62E-02	17
133	GO:0030030	cell projection organization	1.98E-04	1.62E-02	14
134	GO:0019222	regulation of metabolic process	2.00E-04	1.63E-02	41
135	GO:0061061	muscle structure development	2.12E-04	1.71E-02	9
136	GO:0055123	digestive system development	2.23E-04	1.78E-02	5
137	GO:0003413	chondrocyte differentiation involved in endochondral bone morphogenesis	2.26E-04	1.80E-02	3
138	GO:0060191	regulation of lipase activity	2.33E-04	1.84E-02	4
139	GO:0051346	negative regulation of hydrolase activity	2.37E-04	1.86E-02	8
140	GO:0009605	response to external stimulus	2.43E-04	1.88E-02	22
141	GO:0072103	glomerulus vasculature morphogenesis	2.47E-04	1.88E-02	2
142	GO:0072239	metanephric glomerulus vasculature development	2.47E-04	1.88E-02	2
143	GO:0072104	glomerular capillary formation	2.47E-04	1.88E-02	2
144	GO:0031323	regulation of cellular metabolic process	2.51E-04	1.90E-02	38
145	GO:0080090	regulation of primary metabolic process	2.58E-04	1.93E-02	37
146	GO:0060350	endochondral bone morphogenesis	2.59E-04	1.93E-02	4
147	GO:0030324	lung development	2.62E-04	1.95E-02	6
148	GO:0030323	respiratory tube development	2.83E-04	2.08E-02	6

149	GO:0061041	regulation of wound healing	2.92E-04	2.13E-02	5
150	GO:0001503	ossification	2.97E-04	2.16E-02	6
151	GO:0045785	positive regulation of cell adhesion	2.98E-04	2.16E-02	8
152	GO:0050680	negative regulation of epithelial cell proliferation	3.01E-04	2.16E-02	5
153	GO:0030574	collagen catabolic process	3.04E-04	2.17E-02	3
154	GO:0090288	negative regulation of cellular response to growth factor stimulus	3.11E-04	2.20E-02	5
155	GO:0051171	regulation of nitrogen compound metabolic process	3.18E-04	2.23E-02	36
156	GO:0009968	negative regulation of signal transduction	3.22E-04	2.25E-02	14
157	GO:0071310	cellular response to organic substance	3.33E-04	2.29E-02	20
158	GO:0048566	embryonic digestive tract development	3.34E-04	2.29E-02	3
159	GO:0003417	growth plate cartilage development	3.34E-04	2.29E-02	3
160	GO:0071694	maintenance of protein location in extracellular region	3.45E-04	2.32E-02	2
161	GO:0061439	kidney vasculature morphogenesis	3.45E-04	2.32E-02	2
162	GO:0061438	renal system vasculature morphogenesis	3.45E-04	2.32E-02	2
163	GO:0009636	response to toxic substance	3.48E-04	2.33E-02	7
164	GO:0060255	regulation of macromolecule metabolic process	3.55E-04	2.36E-02	38
165	GO:0050790	regulation of catalytic activity	3.59E-04	2.37E-02	18
166	GO:0030335	positive regulation of cell migration	3.78E-04	2.48E-02	9
167	GO:0065009	regulation of molecular function	3.90E-04	2.54E-02	22
168	GO:0001558	regulation of cell growth	4.03E-04	2.61E-02	8
169	GO:0001655	urogenital system development	4.11E-04	2.64E-02	7
170	GO:0090092	regulation of transmembrane receptor protein serine/threonine kinase signaling pathway	4.12E-04	2.64E-02	6
171	GO:0071417	cellular response to organonitrogen compound	4.15E-04	2.65E-02	9
172	GO:0072224	metanephric glomerulus development	4.59E-04	2.91E-02	2
173	GO:0048518	positive regulation of biological process	4.72E-04	2.97E-02	41
174	GO:0043086	negative regulation of catalytic activity	4.73E-04	2.97E-02	10
175	GO:0052548	regulation of endopeptidase activity	4.83E-04	3.01E-02	7
176	GO:0031214	biomineral tissue development	4.98E-04	3.06E-02	4
177	GO:0110148	biomineralization	4.98E-04	3.06E-02	4
178	GO:2000147	positive regulation of cell motility	5.04E-04	3.09E-02	9
179	GO:0051094	positive regulation of developmental process	5.22E-04	3.18E-02	16
180	GO:0060541	respiratory system development	5.48E-04	3.32E-02	6
181	GO:0031175	neuron projection development	5.86E-04	3.48E-02	10
182	GO:0035581	sequestering of extracellular ligand from receptor	5.88E-04	3.48E-02	2
183	GO:0032964	collagen biosynthetic process	5.88E-04	3.48E-02	2
184	GO:0032429	regulation of phospholipase A2 activity	5.88E-04	3.48E-02	2

185	GO:0003416	endochondral bone growth	5.92E-04	3.48E-02	3
186	GO:0006508	proteolysis	5.93E-04	3.48E-02	13
187	GO:0042542	response to hydrogen peroxide	6.12E-04	3.57E-02	4
188	GO:0010035	response to inorganic substance	6.18E-04	3.58E-02	8
189	GO:0002063	chondrocyte development	6.37E-04	3.67E-02	3
190	GO:0051272	positive regulation of cellular component movement	6.40E-04	3.67E-02	9
191	GO:0008347	glial cell migration	6.84E-04	3.90E-02	3
192	GO:0045926	negative regulation of growth	6.88E-04	3.91E-02	6
193	GO:0051259	protein complex oligomerization	7.05E-04	3.98E-02	9
194	GO:0043588	skin development	7.31E-04	4.06E-02	6
195	GO:0098868	bone growth	7.33E-04	4.06E-02	3
196	GO:1900115	extracellular regulation of signal transduction	7.33E-04	4.06E-02	2
197	GO:1900116	extracellular negative regulation of signal transduction	7.33E-04	4.06E-02	2
198	GO:0010243	response to organonitrogen compound	7.37E-04	4.06E-02	11
199	GO:0040017	positive regulation of locomotion	7.49E-04	4.10E-02	9
200	GO:0051216	cartilage development	8.01E-04	4.37E-02	5
201	GO:0010648	negative regulation of cell communication	8.27E-04	4.49E-02	14
202	GO:0030850	prostate gland development	8.38E-04	4.52E-02	3
203	GO:0023057	negative regulation of signaling	8.59E-04	4.61E-02	14
204	GO:0044092	negative regulation of molecular function	8.81E-04	4.71E-02	12
205	GO:0030195	negative regulation of blood coagulation	8.93E-04	4.71E-02	3
206	GO:0072102	glomerulus morphogenesis	8.94E-04	4.71E-02	2
207	GO:0043589	skin morphogenesis	8.94E-04	4.71E-02	2
208	GO:1901699	cellular response to nitrogen compound	9.14E-04	4.79E-02	9
209	GO:0006935	chemotaxis	9.30E-04	4.85E-02	8
210	GO:1900047	negative regulation of hemostasis	9.51E-04	4.91E-02	3
211	GO:0030282	bone mineralization	9.51E-04	4.91E-02	3
212	GO:0048584	positive regulation of response to stimulus	9.55E-04	4.91E-02	20
213	GO:0042330	taxis	9.68E-04	4.95E-02	8
214	GO:0007548	sex differentiation	9.76E-04	4.97E-02	6

Supplemental Table 9: GOnet/DICE GOBP enrichment of significantly upregulated genes (DEGs) in ECM1+ F-Act cells, relative to ECM1- F-act cells.

Rank	GO_term_def	P	P_FDR_adj	NofGenes
1	extracellular structure organization	5.00E-10	5.32E-06	9
2	extracellular matrix organization	4.50E-09	2.47E-05	8
3	regulation of complement activation	2.29E-06	8.33E-03	3
4	regulation of response to stimulus	4.26E-06	1.16E-02	19
5	cellular component organization	1.90E-05	4.15E-02	21
6	regulation of humoral immune response	2.86E-05	4.64E-02	3
7	cellular component organization or biogenesis	3.38E-05	4.64E-02	21
8	response to wounding	3.54E-05	4.64E-02	6
9	regulation of nitrogen compound metabolic process	4.38E-05	4.64E-02	20
10	myelination	4.69E-05	4.64E-02	4
11	ensheathment of neurons	5.16E-05	4.64E-02	4
12	axon ensheathment	5.16E-05	4.64E-02	4
13	paranodal junction assembly	5.53E-05	4.64E-02	2
14	negative regulation of blood coagulation	6.00E-05	4.65E-02	3
15	negative regulation of hemostasis	6.40E-05	4.65E-02	3
16	negative regulation of coagulation	6.82E-05	4.65E-02	3
17	collagen fibril organization	7.26E-05	4.66E-02	3

Supplemental Table 10: GOnet/DICE GOBP enrichment of significantly upregulated genes (DEGs) in ECM1+ F-SH cells, relative to ECM1- F-SH cells.

Rank	GO_term_def	P	P_FDR_adj	NofGenes
1	extracellular structure organization	6.00E-10	6.86E-06	8
2	extracellular matrix organization	8.80E-09	4.77E-05	7
3	supramolecular fiber organization	7.30E-07	2.65E-03	7
4	membrane raft organization	1.60E-06	4.36E-03	3
5	negative regulation of multicellular organismal process	1.41E-05	2.32E-02	9
6	negative regulation of blood coagulation	2.09E-05	2.32E-02	3
7	negative regulation of hemostasis	2.23E-05	2.32E-02	3
8	response to other organism	2.24E-05	2.32E-02	9
9	response to external biotic stimulus	2.26E-05	2.32E-02	9
10	negative regulation of coagulation	2.38E-05	2.32E-02	3
11	collagen fibril organization	2.53E-05	2.32E-02	3
12	response to biotic stimulus	2.56E-05	2.32E-02	9
13	regulation of body fluid levels	4.44E-05	3.72E-02	5
14	regulation of protein processing	5.65E-05	4.22E-02	3
15	negative regulation of cellular process	5.86E-05	4.22E-02	15
16	regulation of protein maturation	6.20E-05	4.22E-02	3
17	negative regulation of wound healing	7.08E-05	4.28E-02	3
18	membrane raft assembly	7.17E-05	4.28E-02	2
19	multi-organism process	7.46E-05	4.28E-02	11
20	regulation of blood coagulation	9.83E-05	4.77E-02	3
21	regulation of plasminogen activation	1.02E-04	4.77E-02	2
22	regulation of hemostasis	1.02E-04	4.77E-02	3
23	negative regulation of cell population proliferation	1.14E-04	4.77E-02	6
24	regulation of coagulation	1.14E-04	4.77E-02	3
25	positive regulation of biological process	1.15E-04	4.77E-02	17
26	negative regulation of multi-organism process	1.15E-04	4.77E-02	4
27	regulation of protein metabolic process	1.24E-04	4.77E-02	11
28	vesicle organization	1.30E-04	4.77E-02	4
29	fibrinolysis	1.36E-04	4.77E-02	2
30	negative regulation of response to wounding	1.37E-04	4.77E-02	3
31	regulation of proteolysis	1.38E-04	4.77E-02	6
32	regulation of developmental process	1.40E-04	4.77E-02	11

Supplemental Table 11: GOnet/DICE GOBP enrichment of significantly upregulated genes (DEGs) in ECM1+ M1MΦ cells, relative to ECM1- M1MΦ cells.

Rank	GO_term_def	P	P_FDR_adj	NofGenes
1	neutrophil chemotaxis	1.30E-09	8.47E-06	5
2	granulocyte chemotaxis	2.10E-09	8.47E-06	5
3	neutrophil migration	2.30E-09	8.47E-06	5
4	granulocyte migration	4.10E-09	1.12E-05	5
5	myeloid leukocyte migration	1.25E-08	2.72E-05	5
6	leukocyte chemotaxis	2.04E-08	3.71E-05	5
7	organonitrogen compound catabolic process	4.62E-08	7.19E-05	8
8	organic substance catabolic process	1.04E-07	1.42E-04	9
9	leukocyte migration	1.74E-07	2.00E-04	5
10	positive regulation of immune system process	1.96E-07	2.00E-04	8
11	cell chemotaxis	2.02E-07	2.00E-04	5
12	catabolic process	5.06E-07	4.60E-04	9
13	chemotaxis	5.82E-07	4.70E-04	6
14	taxis	6.04E-07	4.70E-04	6
15	regulation of leukocyte chemotaxis	8.85E-07	6.43E-04	4
16	cellular catabolic process	2.40E-06	1.55E-03	8
17	positive regulation of leukocyte migration	2.42E-06	1.55E-03	4
18	regulation of apoptotic process	2.86E-06	1.67E-03	8
19	regulation of immune system process	2.91E-06	1.67E-03	8
20	regulation of programmed cell death	3.20E-06	1.67E-03	8
21	regulation of epithelial cell proliferation	3.22E-06	1.67E-03	5
22	regulation of mononuclear cell migration	5.09E-06	2.48E-03	3
23	regulation of cell population proliferation	5.23E-06	2.48E-03	8
24	negative regulation of neuron apoptotic process	5.99E-06	2.65E-03	4
25	immune system process	6.32E-06	2.65E-03	9
26	regulation of cell death	6.33E-06	2.65E-03	8
27	regulation of leukocyte migration	9.06E-06	3.66E-03	4
28	inflammatory response	9.89E-06	3.85E-03	5
29	positive regulation of response to external stimulus	1.06E-05	3.96E-03	5
30	regulation of chemotaxis	1.16E-05	4.22E-03	4
31	regulation of cell communication	1.49E-05	5.24E-03	10
32	regulation of signaling	1.55E-05	5.28E-03	10
33	negative regulation of neuron death	2.04E-05	6.73E-03	4
34	negative regulation of apoptotic process	2.27E-05	7.19E-03	6
35	positive regulation of cell migration	2.34E-05	7.19E-03	5
36	regulation of response to external stimulus	2.37E-05	7.19E-03	6
37	negative regulation of programmed cell death	2.52E-05	7.43E-03	6
38	positive regulation of leukocyte chemotaxis	2.71E-05	7.61E-03	3
39	regulation of neuron apoptotic process	2.76E-05	7.61E-03	4
40	positive regulation of cell motility	2.83E-05	7.61E-03	5
41	regulation of signal transduction	2.86E-05	7.61E-03	9

42	response to oxygen-containing compound	3.03E-05	7.86E-03	7
43	positive regulation of cellular component movement	3.32E-05	8.23E-03	5
44	regulation of localization	3.32E-05	8.23E-03	9
45	complement receptor mediated signaling pathway	3.41E-05	8.27E-03	2
46	positive regulation of locomotion	3.69E-05	8.56E-03	5
47	negative regulation of cellular process	3.69E-05	8.56E-03	11
48	regulation of cellular component movement	4.10E-05	9.31E-03	6
49	negative regulation of response to stimulus	4.52E-05	1.01E-02	7
50	negative regulation of cell death	4.69E-05	1.02E-02	6
51	regulation of angiogenesis	4.77E-05	1.02E-02	4
52	protein catabolic process	4.85E-05	1.02E-02	5
53	regulation of response to stimulus	6.54E-05	1.35E-02	10
54	regulation of cytokine production	7.13E-05	1.42E-02	5
55	regulation of vasculature development	7.17E-05	1.42E-02	4
56	regulation of biological quality	8.61E-05	1.63E-02	10
57	positive regulation of cellular metabolic process	8.66E-05	1.63E-02	9
58	negative regulation of signal transduction	8.81E-05	1.63E-02	6
59	locomotion	8.85E-05	1.63E-02	6
60	regulation of endothelial cell proliferation	8.98E-05	1.63E-02	3
61	positive regulation of macrophage chemotaxis	9.16E-05	1.64E-02	2
62	response to molecule of bacterial origin	9.62E-05	1.69E-02	4
63	regulation of multicellular organismal process	9.92E-05	1.69E-02	9
64	regulation of neuron death	9.93E-05	1.69E-02	4
65	negative regulation of cytokine production involved in immune response	1.10E-04	1.85E-02	2
66	positive regulation of chemotaxis	1.12E-04	1.85E-02	3
67	negative regulation of biological process	1.21E-04	1.96E-02	11
68	positive regulation of vascular endothelial growth factor production	1.31E-04	2.06E-02	2
69	positive regulation of neutrophil chemotaxis	1.31E-04	2.06E-02	2
70	positive regulation of macrophage migration	1.41E-04	2.20E-02	2
71	negative regulation of cell communication	1.49E-04	2.28E-02	6
72	negative regulation of signaling	1.52E-04	2.28E-02	6
73	positive regulation of granulocyte chemotaxis	1.53E-04	2.28E-02	2
74	defense response	1.71E-04	2.52E-02	6
75	positive regulation of metabolic process	1.74E-04	2.52E-02	9
76	negative regulation of multicellular organismal process	1.80E-04	2.58E-02	6
77	macromolecule catabolic process	1.90E-04	2.69E-02	5
78	cell migration	1.93E-04	2.70E-02	5
79	regulation of macrophage chemotaxis	2.02E-04	2.72E-02	2
80	regulation of vascular endothelial growth factor production	2.02E-04	2.72E-02	2
81	regulation of neutrophil chemotaxis	2.02E-04	2.72E-02	2
82	epithelial tube branching involved in lung morphogenesis	2.29E-04	3.05E-02	2
83	positive regulation of neutrophil migration	2.43E-04	3.20E-02	2

84	negative regulation of immune system process	2.52E-04	3.20E-02	4
85	regulation of cell migration	2.53E-04	3.20E-02	5
86	positive regulation of angiogenesis	2.55E-04	3.20E-02	3
87	negative regulation of production of molecular mediator of immune response	2.58E-04	3.20E-02	2
88	defense response to protozoan	2.58E-04	3.20E-02	2
89	positive regulation of epithelial cell proliferation	3.16E-04	3.84E-02	3
90	response to protozoan	3.21E-04	3.84E-02	2
91	regulation of cell motility	3.21E-04	3.84E-02	5
92	response to chemical	3.27E-04	3.87E-02	9
93	positive regulation of vasculature development	3.39E-04	3.98E-02	3
94	regulation of macrophage migration	3.55E-04	4.11E-02	2
95	cell motility	3.64E-04	4.13E-02	5
96	localization of cell	3.64E-04	4.13E-02	5
97	regulation of neutrophil migration	3.72E-04	4.18E-02	2
98	positive regulation of cell population proliferation	3.78E-04	4.21E-02	5
99	cellular response to lipid	3.83E-04	4.22E-02	4
100	positive regulation of nitrogen compound metabolic process	4.27E-04	4.65E-02	8
101	proteolysis involved in cellular protein catabolic process	4.59E-04	4.96E-02	4
102	regulation of locomotion	4.66E-04	4.98E-02	5

Supplemental Table 12: Full phosphoproteomics mass spectrometry output of ECM1 treated HuCFb cells, only significantly different phosphoproteins proteins shown, relative to controls treated with media alone.

Gene names	Student's T-test p-value C_ECM	Student's T-test q-value C_ECM	Student's T-test Difference C_ECM	fold-change relative to control	Amino acid	Charge	Multiplicity	Position	Proteins	Positions within proteins
MAP1B	0.000	0.000	-4.7712	27.3076	S	3	___2	1256	P46821	1256
ARHGEF11	0.000	0.016	-3.3661	10.3107	S	3	___2	255	O15085	255
ANAPC4	0.001	0.033	-1.9620	3.8960	S	3	___2	779	Q9UJX5	779
ANAPC4	0.000	0.015	-1.8261	3.5459	S	3	___2	777	Q9UJX5	777
MYO9B	0.002	0.048	-1.4654	2.7614	S	3	___1	1972	Q13459	1972
CETN2	0.000	0.028	-1.4351	2.7041	S	3	___1	20	P41208	20
SURF2	0.001	0.038	-1.3832	2.6085	T	3	___1	195	Q15527	195
MAP1B	0.001	0.045	-1.3695	2.5839	S	3	___3	1254	P46821	1254
PTPN12	0.000	0.029	-1.2086	2.3112	T	3	___1	509	Q05209	509
KIFAP3	0.001	0.049	-1.2039	2.3036	S	2	___1	60	Q92845	60
MAP7D1	0.001	0.048	1.2388	-2.3600	S	3	___1	410	Q3KQU3	410
BICC1	0.001	0.051	1.3199	-2.4965	S	2	___2	637	Q9H694	637
KRI1	0.001	0.038	1.3394	-2.5304	S	2	___1	136	Q8N9T8	136
SSH3	0.001	0.039	1.3583	-2.5638	S	2	___1	649	Q8TE77	649
PSMF1	0.001	0.038	1.3659	-2.5775	S	2	___1	153	Q92530	153
TNKS1BP1	0.002	0.053	1.3756	-2.5948	S	2	___1	1533	Q9C0C2	1533
BAG6	0.000	0.033	1.3962	-2.6321	S	2	___1	1117	P46379	1117
CNOT2	0.000	0.032	1.4042	-2.6467	S	2	___1	165	Q9NZN8	165
THRAP3	0.002	0.051	1.5059	-2.8400	S	2	___1	248	Q9Y2W1	248
GBF1	0.001	0.036	1.5352	-2.8982	S	2	___1	1780	Q92538	1780
SLC38A1	0.001	0.041	1.5698	-2.9687	S	2	___1	49	Q9H2H9	49
LIG3	0.001	0.036	1.6024	-3.0366	S	2	___1	242	P49916	242
RBM8A	0.002	0.045	1.6026	-3.0369	S	2	___1	42	Q9Y5S9	42
TBX3	0.000	0.031	1.6360	-3.1079	S	2	___1	438	O15119	438

SRRM2	0.002	0.046	1.6526	-3.1440	T	2	___3	903	Q9UQ35	903
VIM;GFAP	0.001	0.034	1.7873	-3.4518	S	2	___1	339	P08670;P14136	339;305
PRPF38B	0.003	0.050	1.8236	-3.5397	S	3	___1	529	Q5VTL8	529
ARHGEF12	0.001	0.028	2.0181	-4.0504	S	3	___1	309	Q9NZN5	309
SRRM1	0.001	0.033	2.0541	-4.1527	S	2	___1	414	Q8IYB3	414
HECTD1	0.004	0.049	2.1957	-4.5810	S	2	___1	357	Q9ULT8	357
RNPS1	0.004	0.046	2.2128	-4.6359	S	2	___2	139	Q15287	139
RNPS1	0.004	0.045	2.2128	-4.6359	S	2	___2	141	Q15287	141
LEMD2	0.000	0.002	2.5741	-5.9549	S	3	___2	134	Q8NC56	134
DNAJC17	0.002	0.040	2.7030	-6.5116	S	2	___1	112	Q9NVM6	112
TRA2B;TRA2A;SRRM1	0.000	0.012	3.2306	-9.3864	S	2	___3	308	P62995;Q13595;Q8IYB3	282;276;308
TRA2B;TRA2A;SRRM1	0.000	0.011	3.4516	-10.9404	S	2	___3	310	P62995;Q13595;Q8IYB3	284;278;310
SRSF1	0.000	0.008	3.4745	-11.1155	S	2	___3	225	Q07955	225
SRSF1	0.000	0.006	3.4795	-11.1543	S	2	___3	227	Q07955	227

Supplemental Table 13: Fisher's exact test (Perseus software) of GO terms significantly enriched in ECM1 treated HuCFb samples (from phosphoproteomics data) ranked by p-value.

GO Category	GOBP term	Enrichment factor	P value	Benj. Hoch. FDR
GOBP name	regulation of calcium-dependent cell-cell adhesion	234.38	0.004	0.996
GOBP name	positive regulation of calcium-dependent cell-cell adhesion	234.38	0.004	0.996
GOBP name	monocyte chemotaxis	234.38	0.004	0.996
GOBP name	macrophage chemotaxis	234.38	0.004	0.996
GOBP name	centriole replication	117.19	0.009	0.996
GOBP name	mitochondrion transport along microtubule	78.125	0.013	0.996
GOBP name	lamellipodium morphogenesis	78.125	0.013	0.996
GOBP name	establishment or maintenance of monopolar cell polarity	78.125	0.013	0.996
GOBP name	establishment of monopolar cell polarity	78.125	0.013	0.996
GOBP name	establishment of mitochondrion localization, microtubule-mediated	78.125	0.013	0.996
GOBP name	plus-end-directed vesicle transport along microtubule	58.594	0.017	0.996
GOBP name	plus-end-directed organelle transport along microtubule	58.594	0.017	0.996
GOBP name	establishment of mitochondrion localization	58.594	0.017	0.996
GOBP name	establishment of cell polarity	39.062	0.000	0.239
GOBP name	organelle transport along microtubule	39.062	0.001	0.996
GOBP name	Rho protein signal transduction	23.438	0.003	0.996
GOBP name	microtubule-based transport	20.38	0.004	0.996
GOBP name	establishment or maintenance of cell polarity	19.003	0.000	0.996
GOBP name	cytoskeleton-dependent intracellular transport	18.75	0.004	0.996
GOBP name	microtubule-based movement	14.205	0.008	0.996
GOBP name	Ras protein signal transduction	9.9734	0.015	0.996
GOBP name	regulation of cell growth	9.0144	0.018	0.996
GOBP name	nuclear division	8.8443	0.019	0.996
GOBP name	mitosis	8.8443	0.019	0.996
GOBP name	microtubule-based process	7.9003	0.005	0.996
GOBP name	cellular component movement	6.0484	0.002	0.996
GOBP name	cellular component organization at cellular level	2.1769	0.020	0.996

GO Category	GOCC term	Enrichment factor	P value	Benj. Hoch. FDR
GOCC name	photoreceptor connecting cilium	156.25	4.766E-05	0.039
GOCC name	nonmotile primary cilium	66.964	3.294E-04	0.136
GOCC name	cell projection	5.5804	6.674E-04	0.183
GOCC name	cytosol	3.0159	9.597E-04	0.198
GOCC name	primary cilium	33.482	0.001	0.221
GOCC name	cytoskeletal part	4.6137	0.002	0.221
GOCC name	cilium	21.307	0.003	0.391
GOCC name	intraflagellar transport particle	234.38	0.004	0.391
GOCC name	filopodium tip	234.38	0.004	0.391
GOCC name	microtubule associated complex	15.121	0.007	0.527
GOCC name	intracellular	13.787	0.008	0.527
GOCC name	kinesin II complex	117.19	0.009	0.527
GOCC name	cell projection part	6.2223	0.009	0.527
GOCC name	protein complex	2.5476	0.009	0.527
GOCC name	XPC complex	78.125	0.013	0.582
GOCC name	nucleotide-excision repair complex	78.125	0.013	0.582
GOCC name	nuclear ubiquitin ligase complex	78.125	0.013	0.582
GOCC name	anaphase-promoting complex	78.125	0.013	0.582
GOCC name	axoneme part	58.594	0.017	0.695
GOCC name	axoneme	58.594	0.017	0.695
GO Category	**GOMF term**	**Enrichment factor**	**P value**	**Benj. Hoch. FDR**
GOMF name	non-membrane spanning protein tyrosine phosphatase activity	234.38	0.004	0.996
GOMF name	microfilament motor activity	78.125	0.013	0.996
GOMF name	actin-dependent ATPase activity	58.594	0.017	0.996

Supplemental Table 14: ECM1 binding partners were pulled out from a purified HuCFb membrane protein lysate using ECM1 coated His-tag isolation Dynabeads and subject to mass spectrometry. Presented is a list of proteins significantly enriched in ECM1 coated pull-down beads, relative to control beads, ranked by p-value. Two proteins of interest (LRP1 and CTNND1) are bolded in green text.

Rank	Gene names	p-value	fold enriched vs Control
1	ECM1	5.218E-05	197.246
2	ACSL3	3.715E-04	4.078
3	PKM	0.001	1.203
4	SFXN1	0.001	2.240
5	UBR5	0.002	1.226
6	PLOD2	0.002	1.372
7	LAMB1	0.004	1.340
8	PTPN1	0.004	1.287
9	UQCRC1	0.006	1.984
10	SF3B3	0.008	1.692
11	HSPA9	0.009	1.559
12	MYH10	0.011	1.102
13	HNRNPK	0.011	1.848
14	PDHA1	0.012	1.883
15	**CTNND1**	0.012	1.333
16	HNRNPH1	0.014	1.494
17	RPS9	0.014	5.453
18	SEC31A	0.015	1.277
19	LAMC1	0.016	1.196
20	RPS18	0.017	6.266
21	IDH2	0.019	1.134
22	DYNC1I2	0.019	1.494
23	H6PD	0.019	1.232
24	EPB41L2	0.019	1.186
25	ERLEC1	0.020	1.803
26	FAT4	0.021	1.208
27	**LRP1**	0.022	1.271
28	DHX9	0.022	1.465
29	GLG1	0.023	1.376
30	SAFB	0.024	2.710
31	HK1	0.024	1.281
32	NID2	0.025	1.759
33	GNB2L1	0.028	1.250
34	ESYT1	0.029	1.230
35	RPL23	0.029	1.324
36	GOLGB1	0.029	1.632
37	FN1	0.031	1.126
38	EFTUD2	0.031	1.814

39	PSMD12	0.031	2.546
40	PML	0.037	1.206
41	PSMC6	0.037	1.270
42	SF3B2	0.038	1.211
43	HNRNPA0	0.039	1.234
44	IGF2R	0.039	1.345
45	LTBP2	0.040	1.444
46	DDX5	0.040	1.894
47	NUP205	0.040	1.114
48	HLA-B;HLA-C;HLA-H;HLA-E;HLA-A	0.043	1.282
49	GYS1	0.043	1.722
50	CCAR2	0.045	1.136
51	VCAN	0.046	1.288
52	FAM134C	0.046	1.180
53	PCBP1;PCBP3	0.047	1.859
54	STOM	0.047	1.187
55	SRRM2	0.047	1.430
56	GCN1L1	0.048	1.097
57	RAB7A	0.048	1.718
58	PLXDC2	0.049	1.245

Supplemental Methods

Reanalysis of published mouse single-cell RNA-sequencing data post-MI

scRNAseq data (ArrayExpress www.ebi.ac.uk/arrayexpress, accession codes E-MTAB-7376) were reanalysed using the Seurat R package 26, with UMAP dimensionality reduction calculated on the top 25 principal components. Cell labels were assigned using previous characterizations (Farbehi et al., 2019). Differentially expressed genes were calculated using the Seurat Find Markers program with MAST testing 27, with a gene defined as DE if it obtained a Bonferroni-adjusted p-value < 1x10-05 and an absolute log fold-change difference > 0.25. For gene expression correlation analyses with Ecm1, Spearman correlation was calculated using the R co. Test function on log-normalized counts. For comparison of Ecm1 expression with ligand-receptor connections, we used a previous approach for modelling ligand-receptor communication between cell populations in Scrase data (Farbehi et al., 2019). Briefly, using a curated set of ligand-receptor pairs 28, a communication weight between a source (ligand-expressing) and target (receptor-expressing) cell type is calculated according to the fold-change difference of the ligand and receptor expression for the source and target cell populations, respectively, with reference to protein: protein association scores in the STRING database 29. Ecm1 expression was correlated (Spearman's Rho) with the number of outbound high-weighted paths (weight > 1.5) for each cell type.

Protein extraction and quantification

To isolate total protein for use in SDS-PAGE, samples were suspended in RIPA lysis buffer containing Roche complete, Mini, EDTA-free protease inhibitor and Phos STOP phosphatase inhibitor cocktail (Sigma-Aldrich®) and homogenized using a Precellys®24 high-throughput tissue homogenizer as per the manufacturer's protocol. The concentration of protein lysate was quantified via BCA assay using a Pierce BCA Protein Assay Kit (ThermoFisher Scientific) as per the manufacturer's protocol.

RNA isolation and analysis

Cells were treated with ECM1 (20ng/ml) in starving media or were untreated control cells (starving media alone) for either 3 h, 6 h or 16 h; as per the Cell culture procedures in main document. Cells were harvested/collected in 900µl Trizol (LS Reagent, Ambion) and disrupted with mechanical forces. RNA was extracted with Trizol (LS Reagent, Ambion) and purified using RNeasy Mini Kits from Qiagen, including gDNA elimination steps as per the manufacturer's protocol. One µg of RNA was used for the synthesis of cDNA utilizing QuantiTect Reverse Transcription kits (Qiagen) and qPCR was performed with Advanced Universal SYBR Green Supermix (BIO RAD). The following primers were used:

Table SM1: Primers and their sequences used for HuCFb cell qPCR experiments

target	FW primer	REV primer
Tpt1	GGC ATG GTT GCT CTA TTG GA	ATT TCC CCT CCA CGG CTC AA
Tgfb1	ATT CCT GGC GAT ACC TCA GC	ATT TCC CCT CCA CGG CTC AA
Tgfb2	GAG AGG AGC GAC GAA GAG TA	TGA GCC AGA GGG TGT TGT
CXCL1	CAC CCC AAG AAC ATC CAA AG	CTT AAC TAT GGG GGA TGC AGG
Wnt5a	CTT TGG GGA TGG CTG GAA G	GGG TTA TTC ATA CCT AGC GAC
ACTA2	AGC GTG GCT ATT CCT TCG TT	CCC ATC AGG CAA CTC GTA ACT
IL6	TTC GGT CCA GTT GCC TTC TC	GTG AGT GGC TGT CTG TGT GG
Col1a	TCA GAA CAT CAC CTA CCA CTG	CCC CAT TCA TTT GTC TTT TTA
IL1b	GAT AAG CCC ACT CTA CAG CTG	GGC AGA CTC AAA TTC CAG CTT
CCL2	AGC AGC AAG TGT CCC AAA GA	GTG GAG TGA GTG TTC AAG TC
TRAF2	GCT GAC TTG GAG CAG AAG GT	GGA GAA GAT GGC GGG TAT G

Assays were validated by generating standard curves to evaluate the efficiency of each primer set. The specificity of PCR products was analyzed via melt curve and gel electrophoresis. All target and reference genes from cDNA transcripts were measured using quantitative real-time polymerase chain reaction (qPCR), performed on a BIO RAD CFX384 and results were analyzed using the CFX Manager Software. mRNA quantities were normalized using two housekeeping genes Tpt1 and β-actin, and final values calculated using the ΔΔCt method.

SDS-PAGE and immunoblot

SDS-PAGE was performed under reducing conditions. BioRad 4x XT sample buffer (BioRad) and 20x sample reducing agent (Life Technologies) was added to total protein lysate solutions, to a total volume of 30 µL. Samples were then reduced at 90 °C for 10 min and loaded into each well of Precast Bolt 4-12% Bis-Tris Plus Gels (ThermoFisher Scientific). Gels were then placed in a Mini-Gel Tank (Life Technologies) electrophoresis system containing Bolt MES SDS Running Buffer (Life Technologies), and 150V (constant volt) was applied for ~1 h at room temperature (RT), or until the blue sample buffer had sufficiently run out of the gel casing. Gels were then transferred to nitrocellulose membranes. Membranes were blocked with 5% skim milk powder suitable for microbiology (Sigma-Aldrich) in TBS supplemented with 0.01% tween-20 (w/v) (TBS-T) for 1 h at RT. Membranes were then washed once with TBS-T and incubated for 2h at RT or overnight at 4°C with primary antibody (Table S2) in 0.5% skim milk in TBS-T. Membranes were washed 3 times in TBS-T then incubated with HRP-conjugated ECL-Anti mouse IgG and ECL-Anti Rabbit IgG (GE Healthcare; 1:5000 dilution) secondary antibodies in 0.5% skim milk in TBS-T for 1 h at RT. Membranes were washed twice with TBS-T, once with TBS, incubated with either Clarity Western ECL Substrate (BioRad), Super Signal West Pico PLUS Chemiluminescent Substrate (ThermoFisher Scientific), or Super Signal West Femto Maximum Sensitivity Substrate (ThermoFisher Scientific) and then imaged using a ChemiDoc Touch Imaging System (BioRad). Immunoblots were analyzed using Image Studio software (Lite version 5.2) to return a numerical value based on band density/intensity, to be used for quantification of protein expression. All washing and incubation steps above were performed on agitation.

Table SM2: Antibodies used.

Antibody Name	Cat#	Company	Concentration
ECM1 for Immunohistochemistry (IHC) and immunofluorescence/immunocytochemistry (IF/ICC)	ab126629	Abcam	1:100
ECM1 for immunoblotting	HPA027241	Sigma-Aldrich	1:500
LRP1	37-7600	Invitrogen	1:200
Vimentin	Ab45939	Abcam	1:1000
Alpha-smooth muscle actin	14-9760-82	Invitrogen	1:500
CTNND1 for immunoblotting and IF/ICC	33-9600	ThermoFisher	1:1500 (immunoblotting), 1:200 (IF/ICC)
Phospho-CTNND1 (s268)	PA5-77935	ThermoFisher	1:1500
Phospho-CTNND1 (s252)	8477	Cell signaling technology	1:500
b-catenin	13-8400	ThermoFisher	1:1000
Active b-catenin	05-665	Sigma Aldrich	1:500
Total-MYPT	PA5-17164	ThermoFisher	1:1000
Phospho-MYPT (Thr696)	5163	Cell signaling technology	1:500
JNK1+JNK2+JNK3	ab179461	Abcam	1:1000
Phospho-JNK1+JNK2+JNK3 (phospho Y185 + Y185 + Y223)	ab76572	Abcam	1:1000
IkB alpha	MA5-15132	ThermoFisher	1:500
NF-κB p65	8242S	Cell signaling technology	1:2000
Phospho-NF-κB p65 (Ser468)	3039S	Cell signaling technology	1:500

Immunofluorescence/Immunocytochemistry

Immunofluorescence/Immunocytochemistry (IF/ICC) was performed on HuCFb cells cultured in Corning® 96 Well Black Polystyrene Microplates (cat# CSL3603). HuCFb cells were cultured under standard conditions until 70% confluent. Media was then removed, cells washed twice with PBS, and fixed in 10% formalin for 15 minutes at room temperature. Cells were washed 3 times in PBS and stored in PBS until IF/ICC protocols commenced.

For IF/ICC, PBS was removed and cell membranes permeabilized with 2% triton x-100 in PBS for 10 minutes at room temperature. Cells were washed 3 times in PBS supplemented with 0.01% Tween-20 (PBS-T), then blocked with Intercept® (PBS) Blocking Buffer (Li-cor; cat# 927-70001) for 1 hour at room temperature. Cells were washed 3 times in PBS-T then incubated with appropriate primary antibodies diluted in Intercept® (PBS) Blocking Buffer supplemented with 0.01% Tween-20, for 1 hour at room temperature. Cells were washed 3 times with PBS-T then incubated with appropriate fluorescent secondary antibodies diluted in Intercept® (PBS) Blocking Buffer supplemented with 0.01% Tween-20, for 45 minutes at room temperature protected from light. Cells were washed 3 times in PBS-T, then incubated with DAPI nuclear stain in PBS-T for 5 minutes. Cells were washed 3 times in PBS-T followed by 2 washes in PBS and imaged with a Cytation3 (BioTek).

To determine the extent of fibroblast-myofibroblast transition, HuCFb cells were cultured to 70% confluence in Corning® 96 Well Black Polystyrene Microplates (cat# CSL3603), cells were incubated with starving media for 16 h, media aspirated, and replaced with starving media containing recombinant human ECM1 (20ng/ml), starving media with no

recombinant human ECM1 (control), or starving media containing both ECM1 (20ng/ml) and recombinant human LRPAP1 protein (RAP, Abcam cat# ab93010) at a 1000x molar excess of recombinant human ECM1, and incubated for 48 hours. LRPAP1 (RAP) is a well-known potent LRP1 cell surface receptor inhibitor.[4,5] Media was then removed, cells washed twice with PBS, and fixed in 10% formalin for 15 minutes at room temperature. Cells were washed 3 times in PBS and stored in PBS until IF/ICC protocols commenced, as detailed above. Fluorescence area of alpha-smooth muscle actin was quantified and normalized to the number of vimentin positive HuCFb cells. Since all cells assayed were vimentin positive, data was presented as sum area of alpha-smooth muscle actin fluorescence/total cell count (DAPI positive nuclei), analyzed with Cytation3 (BioTek) Gen5 software.

Immunohistochemistry (IHC) in human heart failure tissues

Formalin-fixed paraffin-embedded (FFPE) tissue sections to be used in IHC were cut between 2-4µm, mounted onto microscopy slides, and allowed to dry overnight at 37°C.

RNAscope® was conducted according to the RNAscope 2,5 HD Detection Kit (Red) manual, with/without the "Target Retrieval solution" for 15 min (n=2 no retrieval, n=1 retrieval; n=3 total).

For IHC, tissue sections were de-waxed in xylene (2x 10 min), followed by incubation in absolute alcohol for 5 min. Tissue was then rehydrated in a series of 90, 80, 70 and 50% alcohol, followed by one wash in phosphate buffered saline (PBS, pH 7.3) for 5 min. Antigen was unmasked/retrieved by treating with 0.1% Sodium-Citrate-Puffer (pH 6.0) for 40 min at 150 watt in a microwave. Tissue sections were cooled in the antigen retrieval solution for 20 min at RT. Tissue sections were then washed well in 2 changes of distilled water (5 min each) and transferred to PBS. Endogenous peroxidase staining was blocked using 3% H_2O_2 in methanol for 15 min at RT. Sections were washed 3 times in PBS for 3 min each. Antibody was then applied to tissue sections in 1:50 in Dako antibody diluent (cat# S2022) and incubated for 60 min at RT. Tissue sections were washed 3 times in PBS for 3 min each. UltraVision Large Volume Detection Kit was then applied to tissue (Thermo Scientific TL-125-HL) and incubated for 30 min at RT. Sections were then washed 3 times in PBS for 3 min each. Staining was visualized by applying AEC Substrate Chromogen (Ready to use, Dako cat# K3464) and incubated for 10 min at RT. Sections were washed 3 times in PBS for 3 min each and nuclei were counterstained with Mayer´s hematoxylin for 30 sec. Slides were washed in 2 changes of in tap water at 3 min each, and slides mounted with coverslips in Aquatex (Merck cat# 1.08562.0050).

Phospho-proteomics

Cells were lysed in lysis buffer (6M guanidine hydrochloride, 10 mM Tris(2-carboxyethyl)phosphine hydrochloride, 40 mM 2-chloroacetamide in 100 mM Tris-HCl pH 8.5) using a sonication probe at 90% amplitude (counting to 1500 J), reduced, and alkylated for 10 min at 95 °C and centrifuged for 30 min at 3500x*g* and 4 °C to remove cell debris. Protein was precipitated with acetone, resuspended in 4% sodium deoxycholate (w/vol) in 100mM Tris-HCl (pH=8.5) and estimated using the PierceTM BCA Protein Assay. One mg protein was digested with Promega modified trypsin, followed by phosphopeptide enrichment according to Humphrey et al[6] using Venator Sachtopore NP TiO2 beads (SNX

010S003, 3 µm - 100Å, #11110007). Half of each sample was measured in duplicate by nano-HPLC (Dionex Ultimate 3000) equipped with an Aurora Series Emitter nanocolumn with CSI fitting (C18, 1.6 µm, 120 Å, 250 x 0.075 mm; IonOpticks, Melbourne, Australia). Separation was carried out at 50 °C at a flow rate of 300 nL/min using the following gradient, where solvent A was 0.1 % formic acid in water and solvent B was acetonitrile containing 0.1 % formic acid: 0-18 min: 2% B; 18-160 min: 2-25% B; 160-167 min: 25-35% B, 167-168 min: 35-95% B; 168-178 min: 95% B, 178-178 min: 95-2% B; 178-193 min: 2% B. Peptides were detected on a Thermo Orbitrap velos pro mass spectrometer operated in positive ion mode by alternating full scan MS (m/z 300 to 2,000, 60,000 resolution) and MS/MS by HCD of the 10 most intense peaks in the ICR cell with dynamic exclusion enabled. The MS/MS data were analysed for protein identification and label free quantification using MaxQuant 1.6.2.10 against the public database Swissprot with taxonomy *Homo sapiens* and common contaminants (downloaded on 16.04.2019, 20,482 sequences). Carbamidomethylation on Cys was entered as fixed modification, oxidation on Met and phosphorylation on Ser/Thr as variable modifications. Detailed search criteria were used as follows: trypsin, max. missed cleavage sites: 2; search mode: MS/MS ion search with decoy database search included; precursor mass tolerance +/- 4.5 ppm; product mass tolerance +/- 20 ppm; acceptance parameters for identification: 1 % PSM FDR; 1% protein FDR and 1% site decoy fraction. In addition, label free quantitation including the match between runs feature of MaxQuant was performed,[7] requiring a minimum of 2 ratio counts of quantified razor and unique peptides. Data processing was performed using Perseus software version 1.6.5.0, following the proposed workflow for label-free phosphoproteomic data[8]; http://www.coxdocs.org/doku.php?id=perseus:user:use_cases:modifications (last accessed 30/08/2021). Contaminants and reverse phosphorylation sites created during database searches were removed. Intensities were log2 transformed to lower the effect of the outlier values, filtered for a localization probability of >75% and 6 valid values in at least one group, respectively. Missing intensities were replaced with random values taken from the Gaussian distribution of values using default parameters (width of 0.3 and downshift of 1.8), to simulate an intensity value for those low abundant phosphosites. Two-sample t-test with subsequent multiple testing correction by Permutation-based FDR method were used to identify altered phosphorylation sites (s0 = 0.1, FDR = 0.05 with reported q-value and 250 randomizations). For the calculation of signalling scores of averaged group ratios, PHOTON[9] implemented in Perseus version 1.6.5.0 was used, on our ECM1 treated HuCFb phosphoproteomics data as a ratio of ECM1/control with a two-sided PHOTON test, following tutorial data on GitHub (https://github.com/jdrudolph/photon). Protein network data for *Homo sapiens* (v11.0) was downloaded from string database.[10] For all additional gene ontology (GO) enrichment analysis, the GOnet/DICE online tool was used (GOBP, GOCC or GOMF; q-value threshold ≤ 0.05), developed and described by Pomaznoy et al.[11]

Gene ontology testing

For all additional gene ontology (GO) enrichment analysis, “GOnet”/”DICE” online tool was used (GOBP, GOCC or GOMF; q-value threshold ≤ 0.05), developed and described by Pomaznoy et al.[11]

His-tag dependent pull-down of ECM1 protein-protein binding partners

A purified HuCFb membrane/membrane-associated protein lysate was prepared using a Mem-PER Plus Membrane Protein Extraction Kit (ThermoFisher, cat# 89842), as per the manufacturer's protocol. Twenty ug of purified membrane/membrane-associated HuCFb lysate were used per sample. One set of membrane/membrane-associated HuCFb lysate samples (20 ug) were made up to a total volume of 200 µl with either Mem-PER Plus Membrane Protein Extraction Kit solubilization buffer at the supplied concentration (1x detergent samples). A second set of membrane/membrane associated HuCFb lysate samples (20 ug) were made up to 200 µl with a mixture of solubilization buffer and salt buffer to achieve a 1 in 4 diluted detergent concentration (1/4x detergent samples); the salt buffer formulation was 300 mM NaCl, 50 mM Na_3PO_4, pH 7.4. One mg (25 µl) of Dynabeads His-Tag Isolation and Pulldown (ThermoFisher, cat# 10103D) were used per sample and prepared by first washing beads once with His-IP lysis buffer (50 mM Na_3PO_4, 300 mM NaCl, 0.01% Tween-20, 1% Triton x-100, 1x protease inhibitor [Roche, ref# COEDTAF-RO], pH 8) by pipetting beads up and down in solution, followed by placing tubes on a magnetic rack for 1 min to pellet Dynabeads and allow aspiration of wash supernatant. All following bead wash steps were conducted in this manner; similar to the Dynabeads His-Tag Isolation and Pulldown manufacturer's protocol. Washed Dynabeads were then incubation with His-IP lysis buffer containing 500 ng recombinant human ECM1 protein (ECM1 samples; R&D Systems, # 3937-EC-050), or buffer without recombinant ECM1 protein (control/CT samples) for 10 min at RT on constant rotation/inversion. ECM1 and control (no protein) bound beads were then washed 3 times with His-IP wash buffer (50 mM Na_3PO_4, 300 mM NaCl, 0.01% Tween-20, 1x protease inhibitor [Roche, ref# COEDTAF-RO], pH 8) and then incubated with either our previously prepared 1x detergent samples or our 1/4x detergent samples of purified membrane/membrane-associated HuCFb protein lysate, for 45 min at RT on constant rotation/inversion. After 45 min, protein-protein interactions were covalently crosslinked by adding 2.88 µl of a 12.5 mM BS3 (ThermoFisher, cat# 21580) solution (in milli-q H_2O) to the bead-HuCFb lysate sample solution (a ~20x molar excess of BS3, relative to HuCFb protein, was used). The resulting BS3-bead-HuCFb sample solutions were allowed to incubate for 30 min at RT on constant rotation/inversion to achieve protein-protein crosslinking. BS3 crosslinking reactions were then quenched by addition of 8.2 µl of 0.5 M Tris (in milli-q H_2O, pH 7.5) to achieve a final concentration of 20 mM and were incubated for 15 min at RT on constant rotation/inversion. Beads were then washed 3 times in His-IP wash buffer. The resulting purified crosslinked protein-protein complexes were then eluted from Dynabeads by resuspending beads in 30 µl of electrophoresis sample buffer containing BioRad XT sample buffer (BioRad) and XT sample reducing agent (Life Technologies), followed by reducing at 90 °C for 10 min. Eluted samples in reduced buffer were then aspirated off Dynabeads and directly loaded into Precast Bolt 4-12% Bis-Tris Plus Gels (ThermoFisher Scientific), in a Mini Gel Tank (Life Technologies) electrophoresis system containing Bolt MES SDS Running Buffer (Life Technologies). 150 V (constant volt) was applied until the blue Coomassie dye front had migrated sufficiently into the tip 1-2cm of the gel. Gel bands containing gel filtered BS3 crosslinked protein-protein binding complexes were then carefully cut out (below the foot of the loading well but above the Coomassie dye front) and stored in 20% ethanol in milli-q H_2O (w/v) at -20 until in-gel digestion for proteomics.

In-gel proteomics digestion and mass spectrometry of samples from His-tag dependent pull-down of ECM1 protein-protein binding partners

Gel bands from the 12% Bis-Tris Plus Gel were reduced, alkylated and digested with Promega modified trypsin according to the method of Shevchenko et al.[12] Resulting Peptides were acidified with formic acid (final concentration of 0.1%) and analyzed by nano-HPLC (Dionex Ultimate 3000) equipped with an Aurora (Ionoptics) nanocolumn (C18, 1.6 µm, 250 x 0.075 mm). Separation was carried out at 50 °C at a flow rate of 300 nL/min using the following gradient, where solvent A is 0.1% formic acid in water and solvent B is acetonitrile containing 0.1% formic acid: 0-18 min: 2% B; 18-100 min: 2-25% B; 100-107 min: 25-35% B, 107-108 min: 35-95% B; 108-118 min: 95% B, 118-118 min: 95-2% B; 118-133 min: 2% B. A maXis II ETD mass spectrometer (Bruker) was operated with the captive source in positive mode with following settings: mass range: 200-2,000 m/z, 4 Hz, capillary 1,600 V, dry gas flow 3 L/min with 150 °C, nanoBooster 0.2 bar, precursor acquisition control top20 (CID). The LC-MS/MS data were analyzed using Data analysis software (Bruker) with the Sum Peak algorithm, and by MaxQuant 1.6.1.0 by searching the public Swissprot database with taxonomy *Homo sapiens* and common contaminants (downloaded on 16.04.2019, 20482 sequences). Carbamidomethylation on Cys was entered as a fixed modification and oxidation of methionine as a variable modification. Detailed search criteria were used as follows: trypsin, max. missed cleavage sites: 2; search mode: MS/MS ion search with decoy database search included; precursor mass tolerance +/- 0.006 Da; product mass tolerance +/- 80 ppm; acceptance parameters for identification: 1% PSM FDR; 1% protein FDR. Data processing was performed using Perseus software version 1.6.6.0. Contaminants and reverse protein sequences created during database search were removed. Intensities were log2 transformed to lower the effect of the outlier values, filtered for 3 valid values in at least one condition and normalized on the median of each column (by subtraction). For protein groups missing values an imputation step was performed. Briefly missing values were replaced with random values taken from a shifted Gaussian distribution of all valid values (width of 0.3 and downshift of 1.8 separately for each column), to simulate an intensity value for those low abundant protein groups. For statistical analysis, a Two-sample t-test was performed to identify significantly enriched proteins in the ECM1 bound samples (p-value ≤ 0.05); the p-value was not adjusted by multi-testing correction (since otherwise no significant results were left) (**Supplemental Table 14**).

Rac1,2,3 and RhoA G-LISA assay

G-LISA assays to Rac1,2,3 (cat# BK125) and RhoA (cat# BK124) were sourced from Cytoskeleton and performed as per the manufacturer's protocols on HuCFb cells cultured in 6-well plates. Cells were incubated with starving media for 16 h, media aspirated, and replaced with starving media containing recombinant human ECM1 (20ng/ml), or starving media with no recombinant human ECM1 (control) for 10 minutes. Cell lysates were extracted, protein concentration estimated, and lysates subject to G-LISA assay as per manufacturer protocols.

MTT assay

Cell Proliferation Kit I (Roche, Cat# 11 465 007 001) MTT assay was conducted on HuCFbs cultured in Greiner CELLSTAR® 96-well plates (cat# M0562) performed as per the

manufacturer's protocol with readout time-points of 24, 48 and 72 hours; starving media was supplemented with 10% FBS instead of 0.5% FBS.

Wound healing assay

HuCFbs wound healing assays were cultured in Ibidi® culture-inserts (cat# 80369), inserted into each well of a 12-well cell culture plate (ThermoFisher, cat# 150628). Cells were incubated with starving media for 16 h, Ibidi® culture-inserts removed, media aspirated, and replaced with starving media containing recombinant human ECM1 (20ng/ml), or starving media with no recombinant human ECM1 (control). Phase contrast images of the cell gap were acquired hourly at 5x with a Zeiss Cell Observer microscope. Collected images were analyzed where the mean of all 4 positions per well were plotted, and rate of migration per each hour calculated. An equation was fitted over the plotted functions and the inclination (slope) during the 24-hour active migration phase was calculated and compared between control and ECM1 treated groups. For visualization, analysis was also conducted on group dependent differences in the change in rate of migration over time between control and ECM1 using two-way ANOVA by first normalizing the growth rate of all replicates/samples to be equal at time zero.

References

1. Litviňuková M, Talavera-López C, Maatz H et al. Cells of the adult human heart. Nature 2020;588:466-472.
2. Alexanian M, Przytycki PF, Micheletti R et al. A transcriptional switch governs fibroblast activation in heart disease. Nature 2021;595:438-443.
3. Farbehi N, Patrick R, Dorison A et al. Single-cell expression profiling reveals dynamic flux of cardiac stromal, vascular and immune cells in health and injury. eLife 2019;8:e43882.
4. Prasad JM, Migliorini M, Galisteo R, Strickland DK. Generation of a Potent Low Density Lipoprotein Receptor-related Protein 1 (LRP1) Antagonist by Engineering a Stable Form of the Receptor-associated Protein (RAP) D3 Domain. The Journal of biological chemistry 2015;290:17262-8.
5. Falach R, Sapoznikov A, Gal Y et al. The low density receptor-related protein 1 plays a significant role in ricin-mediated intoxication of lung cells. Scientific Reports 2020;10:9007.
6. Humphrey SJ, Karayel O, James DE, Mann M. High-throughput and high-sensitivity phosphoproteomics with the EasyPhos platform. Nature protocols 2018;13:1897-1916.
7. Cox J, Hein MY, Luber CA, Paron I, Nagaraj N, Mann M. Accurate proteome-wide label-free quantification by delayed normalization and maximal peptide ratio extraction, termed MaxLFQ. Mol Cell Proteomics 2014;13:2513-26.
8. Tyanova S, Temu T, Cox J. The MaxQuant computational platform for mass spectrometry-based shotgun proteomics. Nature protocols 2016;11:2301-2319.
9. Rudolph JD, de Graauw M, van de Water B, Geiger T, Sharan R. Elucidation of Signaling Pathways from Large-Scale Phosphoproteomic Data Using Protein Interaction Networks. Cell systems 2016;3:585-593.e3.
10. Szklarczyk D, Gable AL, Lyon D et al. STRING v11: protein-protein association networks with increased coverage, supporting functional discovery in genome-wide experimental datasets. Nucleic acids research 2019;47:D607-d613.
11. Pomaznoy M, Ha B, Peters B. GOnet: a tool for interactive Gene Ontology analysis. BMC Bioinformatics 2018;19:470.
12. Shevchenko A, Wilm M, Vorm O, Mann M. Mass spectrometric sequencing of proteins silver-stained polyacrylamide gels. Analytical chemistry 1996;68:850-8.